ATTACHMENT

Technical Letter Report on Failure Prediction of Electrosleeved Tubes under Severe Accident Transients

October 4, 1999

Prepared by
Saurin Majumdar

Argonne National Laboratory
9700 South Cass Avenue
Argonne, IL 60439

Program Manager
Joseph Muscara
USNRC Office of Nuclear Reactor Research

Not found in adams

DF03

Executive Summary

Under severe accident conditions steam generator tubing can be subjected to very high temperatures. In some accident sequences the temperatures of the tubing will be high enough (≈840°C) that even virgin, undegraded tubing can fail. If other primary system components fail prior to the time the steam generator tubing would reach the temperature at which it will fail, the system will vent inside the containment, the primary system will depressurize, and the steam generator tubes will not fail. If the tubes reach failure before another primary system component fails, a bypass event will occur.

Prediction of failure of a complex composite structure like Electrosleeved steam generator tube under severe accident transients is a difficult problem. The Electrosleeve material derives its strength from its nanocrystalline grain structure. At the high temperatures that are anticipated during severe accidents, rapid grain growth occurs, resulting in a loss of strength. When the review of the behavior of Electrosleeve repairs at high temperatures was initiated, only very limited data on the strength of the Electrosleeve material at high temperatures were available. Analytical models were developed to predict failure. The available data were used determine the parameters of the models, but no confirmatory test results were available.

Two approaches for predicting failure of Electrosleeved tubes were developed. The first is an approximate analytical procedure based on a linear damage rule hypothesis analogous to that often used to analyze creep failures. The second is a more mechanistically based approach that accounts for the loss of flow stress due to grain growth. Initial studies showed the failure temperatures predicted by the two approaches were comparable, but the mechanistic model was used for most of the analyses.

After the initial development of the analytical model, FTI provided failure data from six tests on internally pressurized tubes that were subjected to a variety of temperature ramps simulating those expected during the most challenging severe accidents, "high–dry" sequences that can occur when the core melts, the primary side remains at high pressure, and the secondary side is depressurized. The initial comparison of the model and the tests on tubes with showed that the predicted failure temperatures were within 35–70°C of those observed in the experiments. FTI also additional Electrosleeve specimens that were subsequently tested at ANL. Eleven tests were conducted at ANL. The results from these tests were used to refine the input parameters used in the analytical model. Using the refined model and more accurate data on the test geometries, the predicted temperatures in the FTI and ANL tests are within ±15°C of the observed temperatures.

The model predicts that Electrosleeved tubes with throughwall axial cracks ≤ 1 in. and throughwall 360° circumferential cracks in the parent tubes will survive "high–dry" transients based on the temperature histories for such sequences presented in NUREG–1570. Tubes with throughwall axial cracks of any length but crack depths ≤ 90% are also predicted to survive these transients. Electrosleeved tubes with throughwall axial cracks of any length or 360° C circumferential cracks are predicted to survive severe accidents in which the primary system is depressurized significantly, such as SBO sequence with pump seal leakage.

1. Introduction

Prediction of failure of a complex composite material like the Electrosleeved steam generator tubing under severe accident transients is a difficult problem. The Electrosleeve material is almost pure Ni and derives its strength and other useful properties from its nanocrystalline grain structure, which is stable at reactor operating temperatures. However, it undergoes rapid grain growth at the high temperatures that are expected during severe accidents, resulting in a loss of strength and a corresponding decrease in the flow stress. The magnitude of this decrease depends on the time-temperature history during the accident. Low-temperature tensile data on the Electrosleeve material (without the tube) are available, but the available tensile data on Electrosleeve at high temperatures in either the aged or unaged condition are very limited. Initially the assumption was made that there were no experimental failure data available on Electrosleeved tube with cracks. Therefore, analytical models were exclusively relied upon to predict failure of the composite structure with cracks, using the available tensile data to determine the parameters of the models.

Following initial modeling and analysis, Framatome Technologies, Inc. (FTI) provided failure data from six tests on unsleeved and Electrosleeved tubes with and without notches under simulated severe accident loading. In contrast to the prediction by the model that the damaging effect of notch length should level off with increasing notch length, the FTI test data indicated that the failure temperature of the Electrosleeved tube decreased almost linearly with notch length. On the other hand, the failure temperatures of the unsleeved and degraded tubes were predicted quite accurately by the flow stress model for Alloy 600 presented in NUREG/CR-6575. One of the tests was on an undegraded Alloy 600 tube and involved a long hold time at constant temperature, which the flow stress model cannot handle. However, the creep rupture model for Alloy 600 tubing presented in NUREG/CR-6575 predicts the failure time of this specimen within a factor of 2.

Subsequent to their initial tests, FTI has supplied twelve Electrosleeved tube specimens, three of which have 2 in. long throughwall notches for testing at ANL. Eight other specimens were notched by electro-discharge machining at ANL with notch lengths of 0.5, 1, and 3 in., all nominally 100% throughwall of the parent tube. All specimens were tested to failure using a temperature and pressure history that closely simulated those for a station blackout (SBO) with a depressurized secondary side (Case 6). This report describes the basis for the analytical models and shows how they were revised on the basis of the test results. Although the initial model overestimated the failure temperatures of the FTI tests, the failure temperatures were predicted accurately by the revised model. Finally, the models are used to predict failure of Electrosleeved steam generator tubing during postulated severe accidents.

Two approaches were developed for predicting failure of the Electrosleeved tube, both are based on the flow stress failure model, as discussed in NUREG/CR-6575. The first is an approximate analytical procedure based on a linear damage rule hypothesis. The second is a more mechanistically based approach that accounts for the loss of flow stress due to grain growth. The predicted failure temperatures by both approaches led to comparable results. Although the work in NUREG/CR-6575 showed that a creep model gave a more accurate prediction of failure at high temperatures than a flow stress model, insufficient data are available to do a creep analysis of the Electrosleeved tube at the present. However, based on comparison with limited experimental failure data, it is believed that, in the absence of hold times at constant temperature, flow stress models give reasonable estimates of failure

temperatures for Electrosleeved tubes with cracks. The predictions of the relative strength of tubes with and without repairs are probably more accurate than predictions of failure temperatures. The reference geometry considered in this report is a 7/8 in.–diameter, 0.050-in.-wall-thickness Alloy 600 tubing, with a nominal 0.038-in.-thick Electrosleeve.

2. Description of problem

A schematic of an Electrosleeved tube is shown in Fig. 1. Either an axial crack of various lengths or a 360° circumferential crack is assumed to exist through the full thickness of the parent tube wall. During a severe accident, the tube is subjected to a time-varying temperature and pressure (Δp) history. The flow stress failure criteria for both the axial and circumferential cracks can be stated as follows:

$$\sigma_{lig} = H(T, t), \tag{1a}$$

where H is the flow stress (dependent on the temperature history) of the Electrosleeve and σ_{lig} is the ligament stress, which for the two types of crack is given by Eq. 1b

$$\sigma_{lig} = \begin{cases} m_p \sigma_h \text{ for axial cracks} \\ \sigma_A \text{ for circumferential cracks} \end{cases} \tag{1b}$$

where m_p, which depends on the axial crack length and depth, is the ligament stress magnification factor, σ_h is the hoop stress (calculated using the mean radius and total thickness of the tube and the sleeve) and σ_A is the axial stress based on net section of the tube and the sleeve.

2.1 Determination of m_p for axial cracks

Initially the hoop stress magnification factor m_p for the crack tip ligament in the Electrosleeve was estimated from the equation for a single-layer shell used in NUREG/CR-6575. However, the m_p factor could be reduced if the flow stress of the Electrosleeve ligament is significantly lower than that of the parent tube. In fact, detailed analyses of available tensile data of the Electrosleeve (to be discussed later) showed that, at the temperatures of interest, the flow stress ratio between the parent tube and the Electrosleeve varies between 2-3. To determine the effect of the flow stresses of the Electrosleeve and Alloy 600 on m_p, a series of finite element analyses (FEA) was conducted for a bi-layer tube with a 100% throughwall crack in the outer layer (simulating Alloy 600) under a constant temperature and increasing pressure loading. The ratio between the flow stress of the outer layer and the inner layer (simulating the Electrosleeve) was varied between 1 and 3. The results, plotted in Figs. 2 a-b, confirm that the values of m_p are indeed reduced significantly when the flow stress ratio is increased. The m_p factor as computed from FEA results generally varies with pressure. However, the behavior is different for long cracks as opposed to short cracks, as shown in Figs. 2 a-b. For long cracks, m_p increases with pressure and tends to level off at higher pressure. The behavior for the shorter 0.5 in. crack is just the opposite; it decreases with pressure and tends to level off at higher pressure. However, in both cases, the m_p factor increases rapidly (suggesting onset of failure) with further increase in pressure in a regime where the Electrosleeve experiences significant plastic yielding away from the crack tip ligament. The values of m_p at the point where it levels off (i.e., just prior to failure) were used in the failure models. As shown in Fig. 3,

the m_p obtained from FEA (for flow stress ratio = 1) agrees well with that calculated with the ANL correlation for cracks ≤ 1 in., but levels off with increasing crack length beyond 2 in. On the other hand, the m_p calculated by the ANL correlation continues to increase with increasing crack length, although the actual increases are small beyond a crack length of 2 in.

Note that the m_p factor for the 0.5 in. crack can drop below 1 for an Electrosleeve if the decrease in flow stress is large. Although m_p is decreasing with increasing pressure for short crack, the average ligament stress (or plastic strain) is still increasing with increasing pressure because m_p is obtained by dividing the average ligament stress by the nominal hoop stress in the uncracked section. Nor does a value of $m_p < 1$ imply that the Electrosleeve/Alloy 600 composite tube wall away from the crack will fail before the crack tip ligament. The average stress in the Electrosleeve ligament relative to its flow stress always remains higher than the average stress in the Electrosleeve/Alloy 600 composite tube wall (away from the crack section) relative to its thickness-weighted flow stress.

Because the FEA grid may not have been sufficiently fine to obtain highly accurate solutions, the FEA results were used to calculate the ratio between the m_p for the Electrosleeved tube and the homogeneous tube as a function of the ratio between the flow stress of the parent tube and the Electrosleeve, as shown in Fig. 4. This m_p ratio was then used to scale the m_p calculated by the ANL correlation for a homogeneous tube to obtain the effective m_p of the Electrosleeved tubes with notches as indicated in Eq. 2 (FSR denotes flow stress ratio):

$$m_p(\text{eff.}) = \frac{m_p(\text{FEA})}{m_p(\text{FEA, FSR} = 1)} \times m_p(\text{ANL}) \qquad (2)$$

3. Material properties data for Electrosleeve

The initial development of the model was based on three sets of material properties data contained in a report by Framatome Technologies, Inc. (FTI) entitled, "Electrosleeving Qualification for PWR Recirculating Steam Generator Tube Repair," Report No. BAW-10219P, Rev. 03, October 1998. Subsequently, FTI provided two additional sets of data; one describing the time-dependent decrease in flow stress of the Electrosleeve material upon isothermal aging and the other on failure tests on Electrosleeved tubes with cracks under simulated severe accident transients.

The FTI data show that the Electrosleeve material is stronger than the tube material at the reactor operating temperature. However, at high temperatures (≥400°C), the Electrosleeve begins to lose its hardness because of grain growth (Fig. 5). The thermal aging effect is a complicated phenomenon consisting of at least two steps. In the first step, the phosphide precipitates in the grain boundary, which prevent grain growth, are dissolved, and in the second step grain growth occurs. The starting or initial hardness of the FTI isothermal aging specimens show a very large specimen-to-specimen scatter. Therefore, the loss of hardness data for each specimen was normalized with respect to its initial hardness, as shown in Fig. 5. The data in Fig. 5 suggest that the hardness of the material starts to decrease, albeit at a relatively slow rate, starting very early. The nucleation times for this process for specimens aged at > 425°C are relatively short and are ignored in the nucleation model to be discussed later. The data in Fig. 5 also suggest the existence of a second process with longer nucleation times that involves very rapid decrease in hardness with time and is very likely linked to the

process of rapid grain growth. The reciprocal of the incubation time for the onset of rapid loss of hardness (rapid grain growth) has a temperature-dependent activation energy as shown in Fig. 6. For analyses of loss of hardness, the continuously varying activation energy curve Q was replaced by the step function indicated in Fig. 6. Sensitivity studies, which are presented later in the report, showed that the results are not sensitive to the form chosen for Q.

Data for the yield and ultimate tensile strengths of the Electrosleeve material are given in the FTI report from room temperature to 343°C (650°F). The flow stress, which is the average of the yield and ultimate tensile strengths, as a function of temperature is shown in Fig. 7. The single high temperature Electrosleeve data point in Fig. 7 was estimated from a tensile test conducted on aged material and will be discussed later. Initially, in the absence of any other flow stress data at high temperature, the solid line in Fig. 7 was used as an estimate for the unaged flow stress curve of the Electrosleeve. It should be remembered that, during a severe accident, the actual flow stress of the Electrosleeve is reduced from the unaged curve (H_i) shown in Fig. 7 because of grain growth. The high temperature tests conducted by ANL (to be discussed later) and FTI suggested that the unaged flow stress of the Electrosleeve material is less than that shown in Fig. 7.

FTI also submitted to the NRC data from a series of tensile tests at 343°C on specimens that were exposed to isothermal pre-aging treatment at high temperatures for various times (Fig. 8). The data at 760°C is for a tensile test that was conducted at 760°C. This particular specimen was heated at a slow linear ramp of ~ 5.8°C/min from 327°C. The effective aging time at 760°C was estimated from an activation energy of 35 kcal/mole to be 39 min.

FTI also provided failure data from six tests on internally pressurized tubes that were subjected to a variety of temperature ramps simulating those expected during SBO accidents. The initial temperature ramp rate up to ~ 500°C varied between 3- 5°C/min, which was generally followed by a ramp rate of 7- 9°C/min until failure. However, in some cases the ramp rate was gradually decreased to 1.2 °C/min above 705°C. Three tests were conducted on unsleeved Alloy 600 tubes with and without any degradation and three on Electrosleeved tubes (7/8 in. Dia.) with 0.5, 1 and 2 in. throughwall axial notches in the parent tube.

4. Analytical models

Two analytical models were originally developed for estimating the failure temperature under severe accident transients – a model based on linear damage rule and a model based on the Hall-Petch relationship. In both models, a basic assumption is the existence of a temperature-dependent unaged (i.e., without grain growth) flow stress curve of the Electrosleeve. This unaged flow stress curve is largely a theoretical construct of the models because to establish it directly from tensile tests at high temperatures would be difficult due to the grain growth that would occur in the specimens unless the specimens could be heated up, stabilized, and tested very rapidly. Therefore, it was calculated from high temperature failure data using the models. Ideally, high temperature failure tests on specimens subjected to severe accident temperature and pressure ramps should be used to derive the flow stress curve of the Electrosleeve. Since such test data were not available when the models were first developed, the unaged flow stress curve of the Electrosleeve was derived initially from analyses of the FTI tensile test data on specimens pre-aged at 760°C. Subsequently, the flow stress curve of the Electrosleeve was recalculated on the basis of high temperature failure tests conducted at ANL.

Both models gave comparable results for failure temperatures. Since the Hall-Petch model was more mechanistically based, it was selected for use in failure prediction.

4.1 Model based on Hall-Petch equation

In this model the "nucleation" phase is explicitly separated from the "growth" phase of the grain growth phenomenon. As mentioned earlier, it was assumed that the Electrosleeve has an initial "unaged" flow stress curve $H_i(T)$, e.g., Fig. 7. The hardness or flow stress (at a sufficiently high strain rate) of the Electrosleeve material was assumed to depend on the grain size by the Hall-Petch relationship, i.e.,

$$H(T) = Ad^{-n}f(T), \tag{3}$$

where H(T) is the flow stress at any temperature T, d is the grain diameter, n is the Hall-Petch exponent, and f(T) is a correction factor for temperature. During high temperature exposure, the growth rate of grain diameter was assumed as Eq. 4.

$$\dot{d} = \begin{cases} 0 \text{ for } t < t_n \\ \dfrac{B}{d}\exp\left(\dfrac{-Q_g}{RT}\right) \text{ for } t \geq t_n \end{cases}, \tag{4}$$

where t_n is the nucleation time to loss of flow stress (i.e., onset of grain growth), B is a constant, Q_g is the activation energy for grain growth, R=1.987 cal/mole/°C. Recrystallization due to plastic straining was ignored. The form of the grain growth rate equation was chosen such that, under isothermal aging, the grain growth follows a parabolic law. Under isothermal aging, the reciprocal of the nucleation time ($1/t_n$), which has an activation energy Q_n, is given by the following equation:

$$\frac{1}{t_n} = C\exp\left(\frac{-Q_n}{RT}\right) \tag{5}$$

where C is a constant. The variation of Q_n with T is given in Fig. 6.

The tensile data reported by FTI on pre-aged specimens of Electrosleeve material were used to calculate the values of various parameters in Eqs 3-5. Integrating Eq. 4, using Eq. 5 and assuming $Q_n = Q_g = Q$,

$$d(t) = \left[d_i^2 - \frac{2B}{C} + 2Bt\exp\left(\frac{-Q}{RT}\right)\right]^{1/2}, \tag{6}$$

where d_i is the grain diameter of the as-received material and T is the aging temperature. Substituting Eq. 6 into Eq. 3, denoting the tensile testing temperature as T_o, the initial "unaged" flow stress at T_o as H_o and solving,

$$t\exp\left(\frac{-Q}{RT}\right) = \frac{d_i^2}{2B}\left[\left(\frac{H_o}{H}\right)^{2/n} - 1\right] + \frac{1}{C}, \tag{7a}$$

where

$$H_o = Ad_i^{-n} f(T_o). \tag{7b}$$

Results from the FTI tensile data (T_o=343°C) on pre-aged specimens are plotted in Figs 9a and 9b for assumed values of n =0.33 and n=0.4, respectively. Both fits are quite good and reasonably close to the conventional value of 0.5. Values of $d_i^2/2B$, and $1/C$ were obtained from the slope and intercept of the linear fits. As mentioned earlier, the specimen that was aged for 30 min at 760°C was also tensile tested at 760°C. Since this specimen was ramped from 327°C to 760°C at the slow rate of 5.8°C/min prior to constant temperature aging, an analysis using an activation energy of 35 kcal/mole gave an effective aging time at 760°C of 39 min A reduction factor for the flow stress at 760°C compared to that at 343°C was obtained by fitting the data, excluding the 760°C data, and extrapolating the best-fit line to the value of the time-temperature parameter of the test, as shown by dotted lines in Figs 9a-b. The two flow stress curves, shown in Figs 7 and 10, correspond to the two estimated values of flow stresses at 760°C by the two fits. The difference between the two flow stress curves is negligible.

Nucleation times to onset of loss of flow stress (i.e., grain growth) under isothermal aging were calculated using Eq. 5 and the step-wise varying approximation to the activation energy data shown in Fig. 6. The results, plotted in Fig. 11 for two Hall-Petch exponents, show that the two exponents give widely varying estimates for nucleation times. The nucleation times for the rapid loss of hardness as derived from the FTI data (Fig. 5), also plotted in Fig. 11, show that n=0.33 fits the data better. The calculated curves of loss of hardness (for n=0.33 and 0.4) with time under various isothermal aging are compared with the FTI data in Fig. 12. Although the model does not simulate the initial low rate of loss of hardness, it does represent the subsequent rapid loss of hardness reasonably well for both values of n.

Under a variable temperature history, Eq. 5 can be generalized to give the time to nucleation as follows:

$$C\int_0^{t_n} \exp\left(\frac{-Q}{RT(t)}\right)dt = 1 \tag{8}$$

Similarly, Eq. 4 can be integrated to give the grain diameter at any time t

$$d(t) = \begin{cases} d_i & \text{for } t < t_n \\ \left[d_i^2 + 2B\int_{t_n}^{t} \exp\left(\frac{-Q}{RT(t)}\right)dt\right]^{1/2} & \text{for } t \geq t_n \end{cases} \tag{9}$$

Substituting Eqs 8-9 into Eq. 3 and solving for the flow stress H at any time,

$$H(t) = \begin{cases} H_i(t) & \text{for } t < t_n \\ \left[1 + \frac{2B}{d_i^2}\int_{t_n}^{t} \exp\left(\frac{-Q}{RT(t)}\right)dt\right]^{-n/2} H_i(t) & \text{for } t \geq t_n \end{cases} \tag{10}$$

where $H_i(t)$ is the initial "unaged" flow stress at T(t). Ligament failure is predicted to occur when Eq. 1a is satisfied.

5. Initial analytical results

The model using the Hall-Petch equations to represent the changes in the flow stress was used to calculate failure temperatures. The studies in NUREG–1570 showed that the most severe challenge to the integrity of steam generator tube arises from station blackout (SBO) sequences in which the secondary system dries out and the primary system fails to depressurize (a "high–dry" sequence). In this case the Δp across the tube wall is a constant 2.35 ksi. The time–temperature history was taken as bilinear with an initial 5°C/min segment to 670°C, followed by 2°C/min segment until failure (Fig. 13). This temperature ramp is a simplified version of those used in NUREG–1570 for the severe accident tests on flawed tubes without repairs. It is even more conservative than the NUREG–1570 versions because the slower segment starts at a lower temperature. If another primary system component fails before the steam generator tube fails, the system depressurizes and subsequent failure of the steam generator tubes is unlikely. The surge line is probably the limiting primary system component. Based on earlier calculations, it was assumed that the surge line would fail at the time when the tube temperature is 674°C for this bilinear ramp. Subsequent discussions with NRC staff and additional thermo-hydraulic calculations lead to the conclusion that this particular bilinear ramp, which will be referred to in the remainder of the report as the "scoping ramp." is an overly conservative representation of the "high–dry" SBO sequence, and a more realistic time–temperature history was used for most of the calculations. However, because calculations with the different histories are useful for understanding the sensitivity of the failure temperature to ramp rate, the results are still useful. Additional sensitivity studies were done with simple 1°C/min and 5°C/min ramps. Results are reported for both Electrosleeved and unsleeved tubes so that the relative strengths can be compared.

5.1 Results for unsleeved tubes

The data and the flow stress model presented in NUREG/CR-6575 showed that the failure temperature of an unflawed Alloy 600 tube is 840°C which is greater than the temperature corresponding to surge line failure. Thus, an unflawed tube is predicted to survive the scoping ramp.

An unsleeved Alloy 600 tube with the deepest cracks that can survive a Δp equal to 3 times the Δp during normal operation ($3\Delta p_{NO}$) was also considered; for these calculations $3\Delta p_{NO}$ was taken as 3.84 ksi. The maximum depths of 0.5, 1 and 2 in. long cracks that satisfy this criterion are 76.6%, 67.1% and 62%, respectively. The corresponding maximum depth for a 360° circumferential crack is 80%. Note that $m_p = 2.32$ for all these cracks, which will be collectively referred to as the $3\Delta p_{NO}$ crack. For this value of m_p the ligament stress $\sigma_{lig} = 45$ ksi. The corresponding failure temperature for both the axial and circumferential cracks by the flow stress criterion is 681°C (see e.g., Fig. 10), which is greater than the assumed surge line failure temperature (674°C). The creep rupture model, which is more accurate than the flow stress model, predicts a failure temperature of 728°C. Thus the Alloy 600 tube with a $3\Delta p_{NO}$ crack is predicted to survive the scoping ramp.

5.2 Results for Electrosleeved tubes

Figs 14 a-b show the calculated reduction of flow stress of the Electrosleeve during the scoping ramp as well as at 1°C/min for Hall-Petch exponent n = 0.33 and 0.4, respectively. Note that, for each transient, the variations of flow stress with temperature are almost identical

for the two exponents. Further, for each exponent, there is a difference in the flow stress curves initially for the two transients. Although the two curves ultimately converge, the convergence occurs at a much higher temperature than all the predicted failure temperatures.

Figs. 15a-b show the variation of the predicted failure temperatures (for n=0.33 and 0.4) with axial crack length for an Electrosleeved tube with a throughwall crack in the parent tube subjected to the scoping ramp as well as two other constant temperature ramp rates. Note that the predicted failure temperatures corresponding to n=0.33 and n=0.4 differ by ~5°. The predicted failure temperatures under the scoping ramp for all the cracks considered are above 681°C, which is the failure temperature of unsleeved tubes with a 3 Δp_{NO} crack. The same is also true for the slower constant temperature ramp rate of 1°C/min for cracks ≤ 0.5 in.

The variation of failure temperature with the constant temperature ramp rate is shown in Fig. 16 for an Electrosleeved tube with a throughwall 360° circumferential crack in the parent tube. It is evident that the failure temperatures for such a tube under ramp rates >1°C/min (which includes the scoping ramp) exceed 681°C, which is the failure temperature of unsleeved tubes with a $3\Delta p_{NO}$ crack. As before, the differences in the predicted failure temperatures using n=0.33 and n=0.4 are small.

5.3 Predicted versus observed failure temperatures for FTI tests

As mentioned earlier, FTI performed tests on 7/8 in. diameter unsleeved tubes, both degraded and undegraded, and Electrosleeved tubes with 100% deep axial notches in the parent tube. All the tests were conducted under a constant internal pressure = 2.35 ksi and a variety of temperature ramps with the initial rate (at < 500°C) varying between 3 and 5°C/min. Above a temperature of 500°C, the notched Electrosleeved specimens were ramped at 7-9°C/min to failure, except for the test with a 0.5 in. notch. For this test the ramp rate was gradually reduced to 1.2°C/min above 705°C. Failure temperatures were calculated using the temperature ramps for each specimen supplied by FTI. The predicted failure temperatures for the notched unsleeved Alloy 600 tubes were independent of the temperature history. The comparison between the predicted and observed failure temperatures is shown in Table 1 . The details of the notch and tube geometry of the specimens are included in Table 2. The predictions in Table 1 were made using a high-temperature flow stress curve for the Electrosleeve material that was based on limited high-temperature tensile test data provided by FTI. The predictions are in much better agreement with the observed values, if a modified flow stress curve that includes the results of additional ANL tests is used, as will be discussed later.

The predicted failure temperatures overestimate the experimentally observed failure temperatures of the Electrosleeved tubes in all cases. The failure temperatures of the two degraded Alloy 600 tubes were predicted quite well by the flow stress model of NUREG/CR-6575. Note that these two tests are consistent with each other because the m_p value for a 50% deep 2 in. crack is approximately 2, which is also the hoop stress magnification factor for a 50% uniformly thinned tube. The test on undegraded Alloy 600 involved a hold at constant temperature, which the flow stress model cannot handle. However, the creep rupture model presented in NUREG/CR-6575 can predict the failure time within a factor of 2.

6. ANL test results

As mentioned earlier, FTI provided twelve Electrosleeved specimens three of which were notched. Eight additional specimens were notched (≈ 0.0075 in. wide) at ANL by electro-discharge machining. Eleven tests were conducted at ANL. The time temperature history for these tests consisted of holding the pressure constant at 2.35 ksi while ramping the temperature from 300°C to 545°C at 4.2°C/min followed by 12.5°C/min ramp until failure. (Figs. 17a-b). This closely simulates the SBO sequence identified as Case 6RU in NUREG–1570 and is felt to be a more realistic representation of the sequences of interest than the scoping sequence used for the initial analytical studies. For this case the tube temperature is 684°C when the surge line failure occurs. A summary of all the tests conducted by ANL as well as by FTI is given in Table 2. Note that the FTI tests were conducted using different temperature ramps, as discussed in section 5.3.

In all the ANL specimens with 2 and 3 in. long flaws both the unsleeved tubes and the Electrosleeves failed with large flaw openings (fish-mouth). Although the specimens without repairs also failed with a large flaw openings, the Electrosleeve tubes with 0.5 and 1 in. flaws failed without any visible opening. Similar failure modes were also observed by FTI.

Table 1 Observed and initial predictions of failure temperatures for the FTI severe accident tests on unsleeved and Electrosleeved tubes.

	Electrosleeved Alloy 600 tube			Unsleeved Alloy 600 tube		
	0.5 in. 100%TW	1.0 in. 100%TW	2.0 in. 100%TW	2.0 in. 50% TW	50% uniform thinning	Un-degraded
Observed failure temp.	731°C	691°C	611°C	727°C	724°C	82 min*
Predicted failure temp.	766°C	728°C	682°C	738°C	726°C	164 min**

* this test was held at 764°C until it failed after 82 min

** predicted by the creep rupture model of NUREG/CR-6575

6.1 Revised unaged flow stress curve of the Electrosleeve

The failure temperatures for the ANL tests were used to recalculate the unaged flow stress curve of the Electrosleeve material using the Hall-Petch model (with n=0.33) and the effective m_p factors from Fig. 4 and Eq. 1c. The revised flow stress curve is compared with the previously estimated flow stress curve (Fig. 7) in Fig. 18. Note that the revised curve has a different shape and falls below the earlier estimated curve. This revised flow stress curve is used for all failure predictions in the remainder of this paper.

6.2 Predicted failure temperatures

6.2.1 ANL tests

An examination of Table 2 shows that the geometries of the Electrosleeved tubes have some variations. An upper bound to the predicted failure temperatures was obtained by using the following:

Tube thickness = 0.051 in., sleeve thickness = 0.040 in. and notch depth=0.048 in.,

and a lower bound was obtained by using the following:

Tube thickness =0.049 in., sleeve thickness = 0.035 in. and notch depth=0.049 in.

Table 2 Summary of severe accident tests conducted at ANL and FTI on notched Electrosleeved tubes

Test No.	Notch length (in.)	Notch depth (in.)	Tube wall thickness (in.)	Electrosleeve thickness (in.)	Failure temperature (°C)
BTF-21	0.5	0.0490	0.0490	0.0410	807
BTF-13	0.5	0.0492	0.0510	0.0400	806
BTF-4	1.0	0.0482	0.0510	0.0390	722
BTF-10	1.0	0.0500	0.0520	0.0380	724
BTF-14	1.0	0.0490	0.0500	0.0390	714
BTF-19	2.0	0.0490	0.0510	0.0400	680
BTF-22	2.0	0.0495	0.0500	0.0380	653
BTF-20	2.0	0.0490	0.0510	0.0370	653
BTF-18	3.0	0.0503	0.0505	0.0395	643
BTF-17	3.0	0.0493	0.0510	0.0350	630
BTF-5*	3.0	0.0490	0.0490	0.0440	673
BTF-23**	0.5	0.049	0.050	0.035	731
BTF-25**	1.0	0.051	0.051	0.036	691
R.5.2**	2.0	0.051	0.050	0.036	611

*One tip of the notch in this specimen was about 0.1 in. from the end of the Electrosleeve

**these tests were conducted by FTI

In cases where the notch depth was less than the full thickness of the parent tube wall, an effective flow stress for the ligament (average flow stress weighted by thickness) was used. The two bounds together with the test data are plotted in Fig. 19. Both the test data and the model indicate that the decrease in failure temperature with crack length saturates at a notch length of ≈ 3 in. and no significant additional decrease of failure temperature should occur at longer crack lengths. The tube-to tube variations in geometry give rise to a significant

difference between the two bounds, and a much better correlation between the predicted and the observed failure temperatures (±15°C) is obtained if the actual geometry for each specimen is used in calculating the predicted failure temperatures (Fig. 20).

6.2.2 FTI tests

Fig. 21 shows a comparison of the failure temperatures as reported by FTI and the two bounds based on the same geometrical assumptions as in Fig. 19. All the tests tend to fall near the lower bound curve, which is not surprising because the thicknesses of the Electrosleeve were close to the lower bound thickness assumed for the curve. The predicted failure temperatures (using actual geometry and actual temperature ramp) are within 15°C of the observed values. The failure temperatures of the Electrosleeved tubes with throughwall notches appear to vary almost linearly with notch length (the curve is actually slightly concave downwards), as shown in Fig. 21, which is quite different from the predicted concave-upwards shape of the bounds.

Fig. 22 shows typical failure temperature data for Alloy 600 tubes with part-throughwall notches reported in NUREG/CR-6575 together with predicted values using a flow stress model. For the notch depths chosen, the predicted failure temperatures by the flow stress model are close to those predicted by the creep rupture model, which was shown to be the more accurate of the two in NUREG/CR-6575. Note that in all cases the predicted curves, which have been validated with many high temperature tests at ANL, are concave upwards, which is the shape predicted by all other available correlations also. However, as mentioned earlier, the FTI test failure temperatures of the Electrosleeved tubes appear to vary almost linearly with notch length. The difference can be traced to the fact that specimen BTF-23 (0.5 in. notch) had a slower temperature ramp at high temperature (>705°C) while the other two specimens did not. Also, the notch in specimen R.5.2 (2 in. notch) penetrated into the Electrosleeve. The test failure temperatures were adjusted by using the flow stress model so that all specimens had identical (as those of BTF-25) tube wall thickness, Electrosleeve thickness, notch depth and were subjected to the same temperature ramp as was used for specimen BTF-25. The adjusted failure temperature curve is concave upwards, as shown in Fig. 23. Note that the upward shift of the adjusted failure temperature for the 0.5 in. crack specimen (primarily due to adjusting the ramp rate) is much greater than that for the 2 in. crack specimen.

6.2.3 Case 6 (SBO severe accident)

As mentioned earlier, calculations were done for the temperature and pressure histories shown in Figs. 17 a-b that closely simulate Case 6RU of NUREG–1570. Failure calculations were performed for the reference 7/8 in. dia. tube (wall thickness = 0.050 in. and Electrosleeve thickness = 0.038 in.) with 90% and 100% throughwall cracks of various lengths in the parent tube. The results, plotted in Fig. 24, show that failure temperatures for 100% throughwall 3, 2, 1 and 0.5 in. long cracks are 650, 660, 705 and 800°C, respectively. Since the surge line failure occurs when the tube temperature = 684°C, cracks ≤ 1 in. long are predicted to survive the Case 6 transient. If the cracks were 90% rather than 100% throughwall, all would survive the Case 6 SBO severe accident.

6.2.4 *Case 20C (SBO with pump seal leakage)*

The variation of temperature and pressure during an SBO severe accident with pump seal leakage (Case 20C) is shown in Fig. 25. The variations of temperature, ligament flow stress and ligament stresses for various crack lengths with time are plotted in Fig. 26 for the reference 7/8 in. dia. tube (wall thickness = 0.050 in. and Electrosleeve thickness = 0.038 in.) with 100% throughwall cracks. Since none of the ligament stresses exceed the flow stress before surge line failure, tubes with 0.5, 1 and 2 in. cracks are predicted to survive this transient.

7. Sensitivity analyses

7.1 Creep effect

In this report, a flow stress model was exclusively used to predict failure under severe accident transients. However, as was concluded in NUREG/CR-6575, a creep rupture model can predict the failure temperatures under severe accident transients more accurately than a flow stress model. A comparison between the predicted failure temperatures by the two models are shown in Table 3 for the case of an unsleeved tube with a $3\Delta p_{NO}$ crack, i.e., a 0.5 in. by 76.6% or a 1 in. by 67.1% or a 2 in. by 62% crack or a 80% deep 360° circumferential crack.

Table 3 Predicted failure temperatures by flow stress model and creep rupture model for an unsleeved tube with a $3\Delta p_{NO}$ crack subjected to various temperature transients and constant internal pressure of 2.35 ksi.

Ramp rate (°C/min)	Flow stress model (°C)	Creep rupture model (°C)
1	681	683
5	681	728
5 to 670°C then 2	681	707
4.2 to 545°C then 12.5	681	756

Note that the failure temperature predicted by the flow stress model agrees well with that by the creep rupture model for the 1°C/min ramp, but is conservative for the other three ramps. In particular, the faster the ramp rate the more conservative the prediction is. Since the unaged flow stress of the Electrosleeve was calculated from tests which were all conducted using a temperature ramp 12.5°C/min, it is expected that the flow stress model will overestimate the failure temperatures for tests at slower ramp rates unless grain growth effects predominate creep effects. Also, it should be noted that the failure times under constant temperature holds cannot be calculated with the flow stress models presented in this report unless grain growth effects predominate creep effects. To accurately predict failure of Electrosleeved tubes under an arbitrarily varying temperature history including constant temperature holds, a creep rupture model, analogous to that presented in NUREG/CR-6575, coupled with a grain growth model has to be developed.

7.2 Thickness of Electrosleeve

The effect of an increase of Electrosleeve thickness from 0.038 in. to 0.043 in. on the ligament failure temperature under the reference Case 6 SBO ramp is shown in Fig. 27. There is a ~20°C increase in the failure temperature for all crack lengths.

7.3 Crack depth

In most of the analyses to date, the crack depths were assumed to be 100% of the parent tube wall. This is probably the major conservatism in the analysis, since the crack depth will typically be less than this. Since the ligament for a crack that is less than 100% deep is a composite of Alloy 600 and the Electrosleeve material, an area-weighted flow stress was used to predict failure. The predicted failure temperatures, plotted in Fig. 28, show that the increase in ligament failure temperature from that for a 100% deep crack ranges between 35-60°C for a 90% deep crack and 50-100°C for a 80% deep crack, with the larger increases occurring for longer cracks. The stress intensity factor for the preexisting crack would also be greatly reduced by the addition of the overlay which should substantially reduce, if not arrest, subsequent crack growth by fatigue or by stress corrosion. Tests with part-through cracks will be needed to verify the predicted failure temperatures because the area-weighted flow stress was used for calculating not only the failure temperature but also the effective m_p factor.

7.4 Crack length

In all the calculations and tests to date, the maximum crack length considered was 3 in. The test data shown in Fig. 19 clearly suggests a leveling off of the failure temperature with increasing crack length beyond 3 in. However, a question arises as to whether there could be a significant reduction in failure temperature if crack length were much longer. This is particularly of concern because although the m_p values calculated by the ANL correlation and by FEA agree remarkably well for crack lengths $\leq$ 1 in., there is some discrepancy between the two for crack lengths>1 in. (Fig. 3). In Fig. 3, it is evident that, for a flow stress ratio of 1, although the ANL correlation shows a slight increase of m_p from 2.0 to 2.1 as the crack length is increased from 2 in. to 3 in., the FEA shows virtually no change in m_p from 1.85. In a similar fashion, for a flow stress ratio of 2, the FEA shows no increase in m_p from 1.6 when the crack length is increased from 2 in. to 3 in. The FEA results suggest that there should be no change in failure temperature beyond a crack length of 2 in. and the test data in Fig. 19 may be interpreted to support this. On the other hand, ANL correlation implies a further decrease in failure temperature with crack length. To be conservative, the ANL correlation for m_p modified by flow stress correction factors derived from FEA was used. To estimate the magnitude of reduction in failure temperature with crack length, a plot of the ligament failure temperature with crack length up to 6 in. is shown in Fig. 29. Note that the reduction is 5°C in failure temperature going from a crack length of 2 in. to 3 in. and an additional 5°C from 3 in. to 6 in. Thus although the ANL correlation suggests that the failure temperature continuously decreases with increasing crack length, from a practical view point the additional decrease beyond a crack length of 3 in. is negligible.

7.5 Variation of activation energy with temperature

For all analyses in this report, the variation of the activation energy with temperature has been idealized by a step function, as shown in Fig. 6. To check the sensitivity of the calculated flow stress on the shape of the activation energy curve, the step function was replaced by the following:

$$Q = \begin{cases} 70 & T < 400 \\ -45\dfrac{T-400}{150} + 70 & 400 \le T < 550 \\ 35 & T \ge 550 \end{cases}$$

i.e, plateaus at high and low temperature connected by a ramp. Fig. 30 shows that, while the choice of Q does affect the shape of the transition of the flow stress, it seems to have little real effect on the predicted behavior in severe accidents at high temperatures.

7.6 Failure criterion

The failure criterion Eq. 1a was originally developed for cracks in homogeneous single layer shells and has been shown to be valid for a wide variety of ductile materials at low temperatures. FEA calculations for various ligament averaged stresses and plastic strain with pressure in a homogeneous tube with a 0.088 in. wall thickness containing a 3 in. long, 0.05 in. deep crack are shown in Fig. 31. This geometry corresponds to a crack in an Electrosleeved tube with a flow stress ratio = 1. Since the flow stress for the tube was assumed to be 60 ksi, Eq. 1a-b would predict a failure pressure of ~ 8 ksi, which is close to the failure pressure (7 ksi) predicted by the ANL correlation for m_p. Note that the failure pressure correlates better with the average hoop stress rather than with either the average von-Mises effective stress or the average plastic strain in the ligament. In fact, the failure pressure corresponds to a calculated average ligament plastic strain of only ~3%, which is much less than the uniaxial ductility of Alloy 600. However, Fig. 31 shows that the average ligament plastic strain is rising steeply with pressure. This rapid rise of plastic strain with pressure together with the high average hydrostatic stress (which generally reduces ductility) in the ligament are probably the reasons for the success of the criterion. Although different materials may have different uniaxial strains to failure, they would result in only modest changes in the failure pressure.

The corresponding case of a bi-layer tube (simulating an Electrosleeved tube at high temperature) with a flow stress ratio =2 is shown in Fig. 32. Since the flow stress of the softer inner layer (simulating the Electrosleeve) is 30 ksi, the current procedure with Fig. 32 would predict a failure pressure of 4.8 ksi, which again corresponds to an average ligament plastic strain of ~3%. As before, the average plastic strain in the ligament is rising rapidly with pressure at this load level. Fig. 32 shows results (using infinitesimal strain and displacement theory) up to a ligament plastic strain of 25%. A more appropriate finite deformation analysis would have indicated an even more rapidly rising plastic strain with pressure. Thus, even if the ductility of the inner layer (Electrosleeve) is greater than that of the outer layer (Alloy 600), the additional pressure capability of the tube beyond that corresponding to an average ligament plastic strain of 3% would be small. At room temperature where the failure is controlled by time independent plastic deformation, the finite element results suggest that Eq. 1a would be a reasonable failure criterion for Electrosleeved tubes. At high temperatures, tests on notched Alloy 600 tubes have shown that the flow stress criterion is less successful and that failure is

better described by a creep damage criterion, particularly for deep notches (≥80%). But the flow stress model was still reasonably successful for shallower notches (≤66%), and it might be expected that the relative estimates of strength provided by the model are accurate even if the absolute failure temperatures are somewhat less so. Failure temperatures for tests on notched unsleeved and notched Electrosleeved tubes conducted by ANL as well as by FTI have been predicted with reasonable success using the flow stress model except for a single test on an unnotched Alloy 600 tube which was subjected to a constant temperature hold. It is expected that the current flow stress model will overestimate the failure temperatures if the temperature ramp rates are significantly slower than those used in the tests at ANL and if creep effects were to predominate grain growth effects.

7.7 Reduction of flow stress with aging

In this report, aging has been simulated using a grain growth model together with the hardness data supplied by FTI on Electrosleeve specimens aged at 760°C. Thus, there is reason to expect some uncertainty in the calculated loss of flow stress with aging. FTI has suggested that the flow stress of Ni-200 at high temperature should provide a reasonable estimate for the flow stress of Electrosleeve after grain growth. A comparison of flow stress data of Ni-200 and Ni-201 with the calculated flow stress of the Electrosleeve for the Case 6 ramp rate (including the effect of aging) is shown in Fig. 33. The data for Ni-201 extends only to 649°C. The two FTI data points at 593°C and 760°C on aged Electrosleeve fall quite close to the Ni-200 curve. In the temperature range of interest for severe accidents, i.e., >650°C, the calculated aged flow stress curve is close to but a little below the Ni-200 flow stress curve. Note that the FTI data at 760°C on aged Electrosleeve falls below the Ni 200 curve and is closer to the calculated flow stress curve. Thus, the present estimates for loss of flow stress with aging are consistent with the FTI assumption for the severe accident transient.

8. Conclusions

Two flow stress-based models have been developed for predicting failure under expected severe accident transients. Both models account for the loss of flow stress of the Electrosleeve with aging and predict comparable failure temperatures for both axial and circumferential cracks during a postulated SBO transient. The predicted flow stresses after accounting for aging agree reasonably well with those of Ni 200 at high temperatures. The Hall-Petch model, which is the more mechanistic of the two approaches, was adopted for calculating the failure temperatures of Electrosleeved Alloy 600 tubes with axial and circumferential throughwall cracks subjected to two severe accident transients: (1) SBO (Case 6) and (2) SBO with pump seal leakage (Case 20C).

Finite element analyses were conducted to validate the m_p factor used in the model for calculating average ligament stress in single layer shells with part-through axial cracks. The same model showed that the m_p factor for the Electrosleeve ligament in a 100% throughwall axial crack is reduced when the flow stress of the Electrosleeve is reduced compared to that of the parent tube. The reduction is greater for shorter cracks. Therefore, a flow stress and crack length-dependent correction factor was applied to the m_p factor calculated with the ANL correlation that was developed originally for single layer shells.

Eleven high temperature tests simulating an SBO (Case 6) pressure and temperature ramp have been conducted on notched Electrosleeved tubes supplied by FTI. The test results

indicate a leveling off of failure temperature with crack length beyond 2 - 3 in., which is consistent with the FEA results. The flow stress data supplied by FTI together with the ANL test results were used to derive an unaged flow stress curve of the Electrosleeve from room temperature to high temperatures. The unaged flow stress curve was used in the model for predicting failure. All the test data fall within the upper and lower bounds calculated on the basis of limiting geometrical parameters observed in the specimens. Also, high temperature test data on notched unsleeved as well as notched Electrosleeved tubes reported by FTI can be predicted reasonably well by the flow stress model.

Based on model prediction as well as four tests on two different heats of Alloy 600 tubes, undegraded virgin tubes are predicted to survive both severe accident transients. Tubes with the deepest axial and 360° circumferential cracks that meet the 3 Δp_{NO} criterion are predicted to fail during the postulated SBO (case 6) transient at 681°C which is close to 684°C which corresponds to surge line failure. The same cracked tubes are predicted to easily survive the severe accident transient Case 20C until surge line failure.

Electrosleeved tubes with throughwall axial cracks ≤ 1 in. and throughwall 360° circumferential crack in the parent tube are predicted to survive the postulated SBO (Case 6) transient until surge line failure. Tubes with any ≤ 90% throughwall axial cracks in the parent tubes are predicted to survive the same transient until surge line failure. Electrosleeved tubes with throughwall axial and circumferential cracks are predicted to survive the severe accident transient Case 20C until surge line failure.

A sensitivity analysis showed that the predicted failure temperatures are increased significantly if the depth of the crack in the parent tube is ≤ 90% throughwall. They will also increase if the thickness of the Electrosleeve is increased. FEA calculations and ANL tests suggest that the adverse crack length effect should level off at 2-3 in. The model predicts a continuing reduction of failure temperature with increasing crack length. However, the additional reduction in predicted failure temperature from a crack length of 3 in. to 6 in. is only 5°C.

The proposed model with the unaged flow stress curve of the Electrosleeve reported here are valid for temperature ramps that are not significantly different from the ramp rate (12.5°C/min) used in the ANL tests because creep effects are neglected in the model. The rate effect that is predicted by the model is due to grain growth only. Predicted failure temperatures at ramp rates significantly different from 12.5°C/min will be accurate if grain growth effects predominate creep effects.

The ligament rupture criterion based on flow stress of the ligament used in the present report was developed from analyses and tests on part-throughwall cracks in single layer shells. The application of the flow stress criterion to a composite structure using the flow stress of the weaker Electrosleeve without any credit given to the stronger parent tube may be conservative, particularly for a highly ductile material like the Electrosleeve. However, all of the ANL and FTI tests, that did not include constant temperature holds, are consistent with the flow stress failure criterion. If prediction of failure under an arbitrarily varying temperature history is of interest, a creep rupture-based model coupled with a grain growth model may be needed.

Acknowledgement

Helpful discussions with Drs D. R. Diercks and W. J. Shack of Argonne National Laboratory and Dr. J. Muscara of the USNRC are acknowledged. Thanks are also due to Framatome Technologies, Inc. for providing the Electrosleeved specimens and Mr. J. Franklin of Argonne National Laboratory for conducting the high temperature tests.

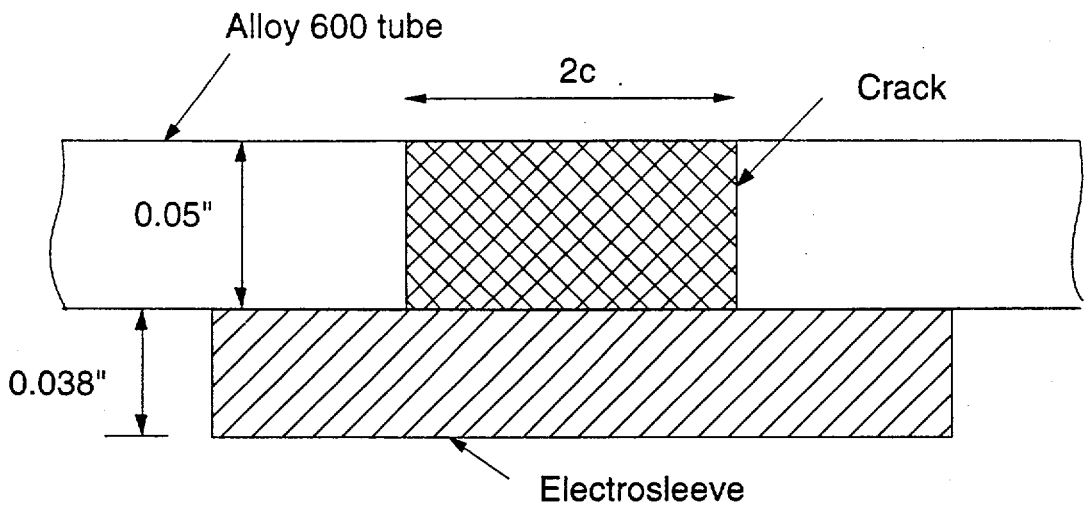

Fig. 1. Reference geometry for Electrosleeved steam generator tube with an axial crack.

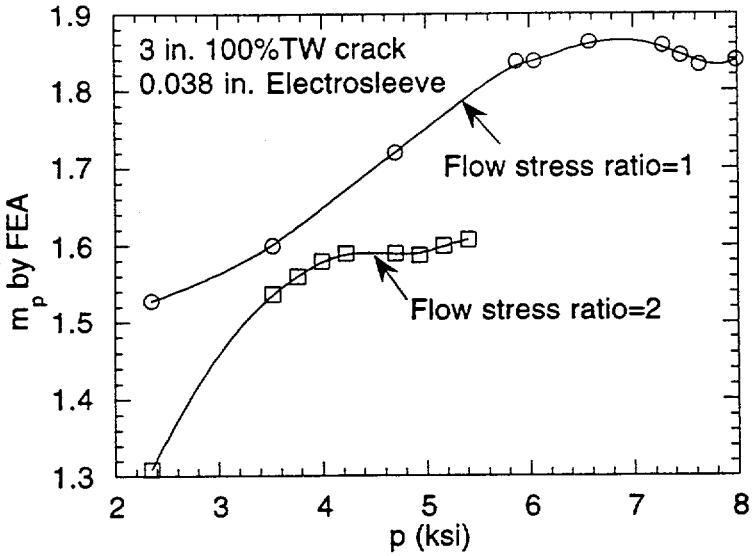

(a)

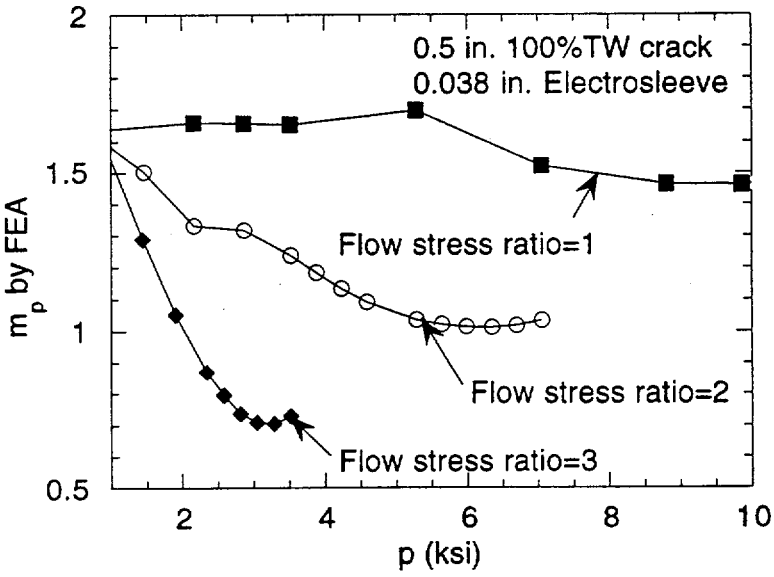

(b)

Fig. 2. Variation of the m_p factor with pressure for (a) 3 in. long and (b) 0.5 in. long cracks for various values of flow stress ratios between the tube and the Electrosleeve.

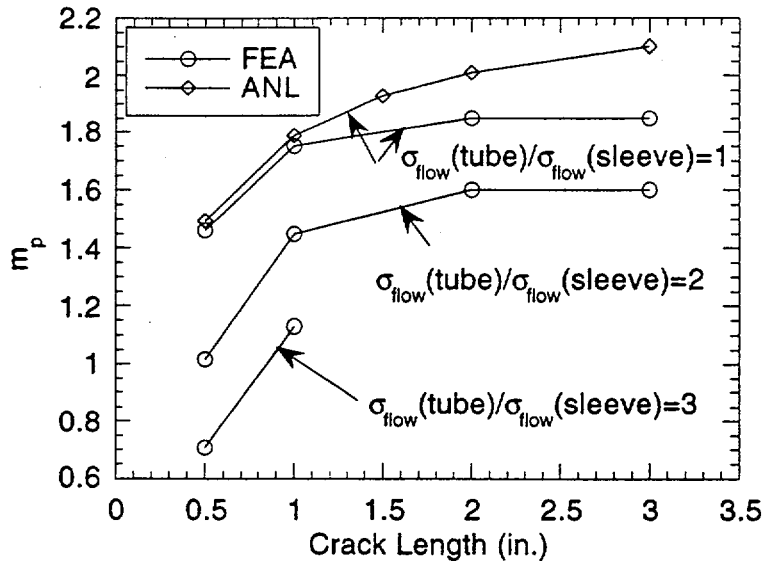

Fig. 3. Comparison of m_p values calculated by ANL correlation with those by FEA for ratios of flow stress of Alloy 600 and the Electrosleeve of 1, 2, and 3. Tube wall and Electrosleeve thicknesses were assumed equal to 0.050 in. and 0.038 in., respectively.

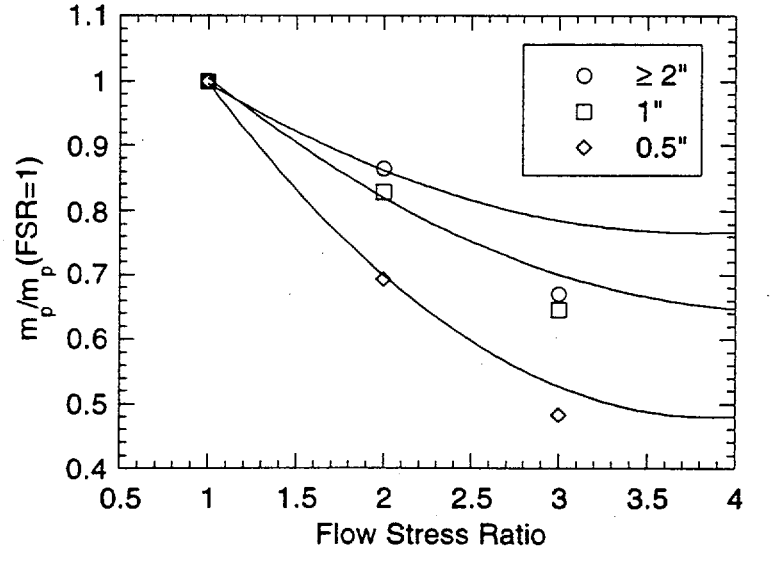

Fig. 4. Variation of the m_p reduction factor with flow stress ratio (FSR) as calculated from FEA results for various crack lengths.

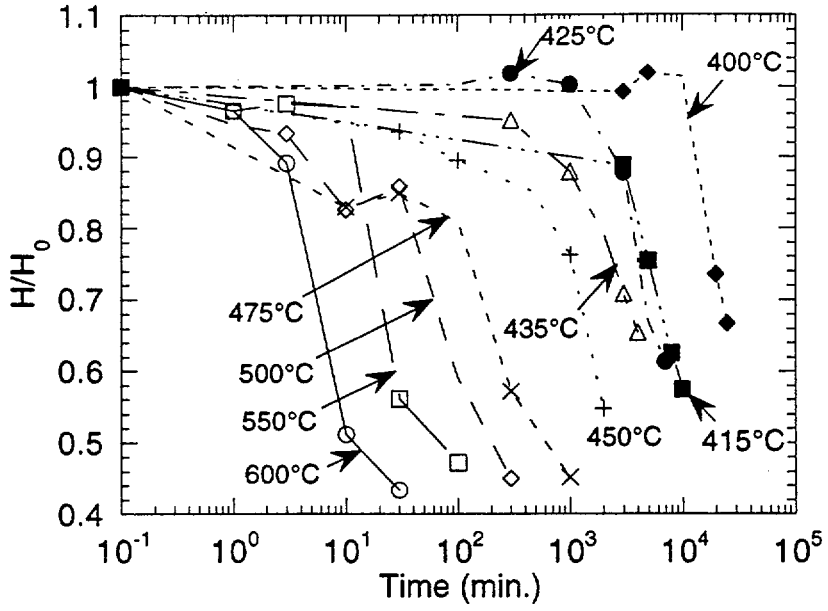

Fig. 5. Variations of normalized Vickers Hardness Number (VHN) of the Electrosleeve material with time under isothermal aging at various temperatures.

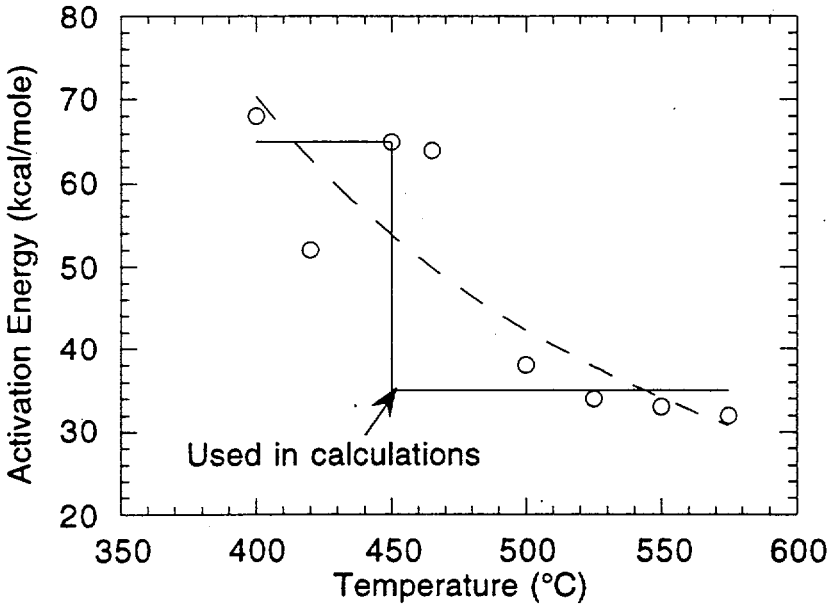

Fig. 6. Variation of activation energy for the reciprocal of the time to onset of rapid reduction of flow stress (or grain growth) with temperature.

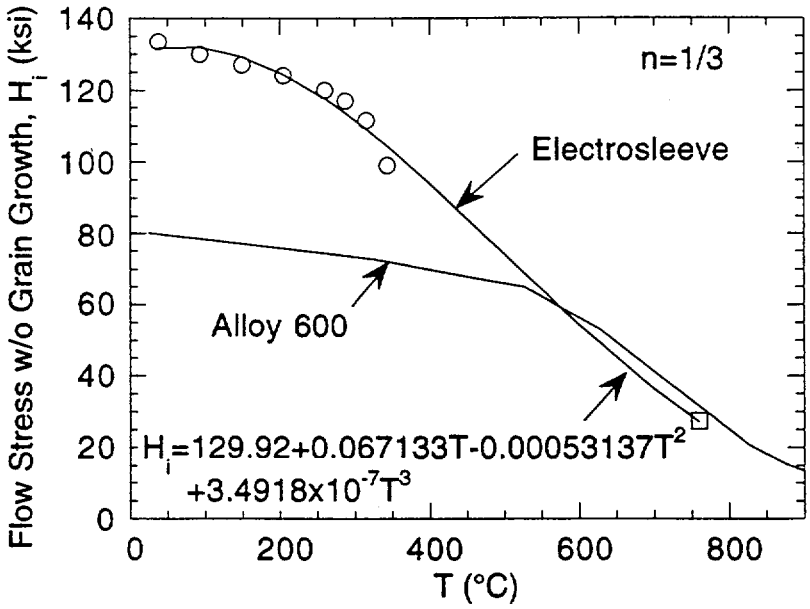

Fig. 7. Flow stress (without aging) vs. temperature plot for electrosleeve material and Alloy 600. The Electrosleeve data (square symbol) at 760°C was estimated from tensile data on a single specimen pre-aged and tested at 760°C, using n=0.33. Note that this flow stress curve of the Electrosleeve was subsequently modified on the basis of ANL tests.

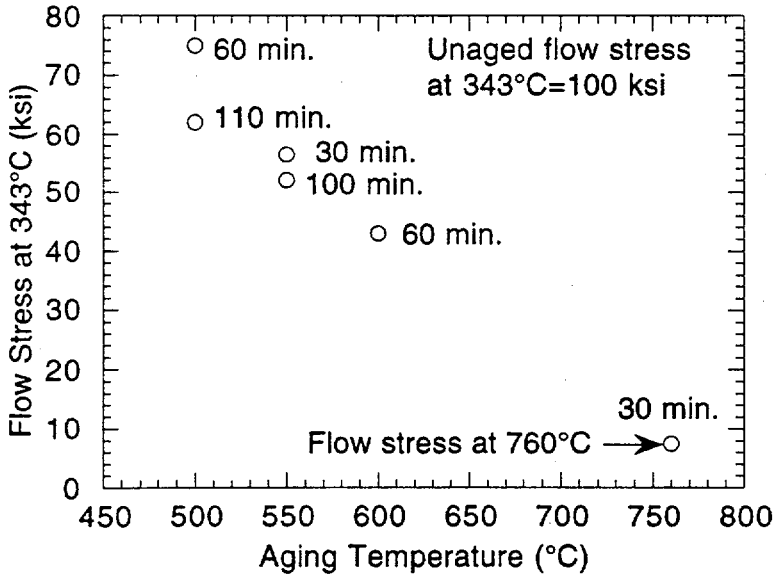

Fig. 8. Flow stress data on the Electrosleeve material pre-aged for various times at high temperatures. All the tensile tests were conducted at 343°C, except for the test on the specimen pre-aged at 760°C, which was conducted at 760°C.

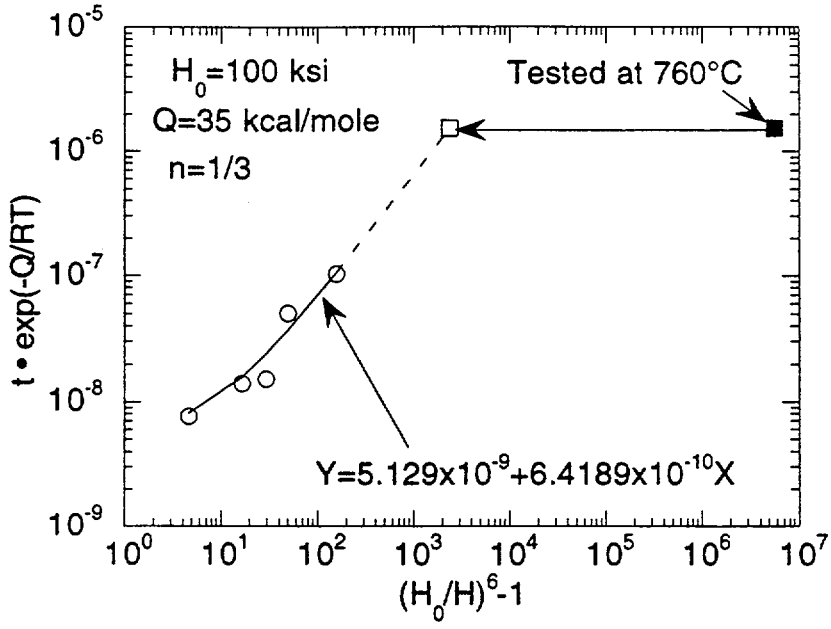

(a)

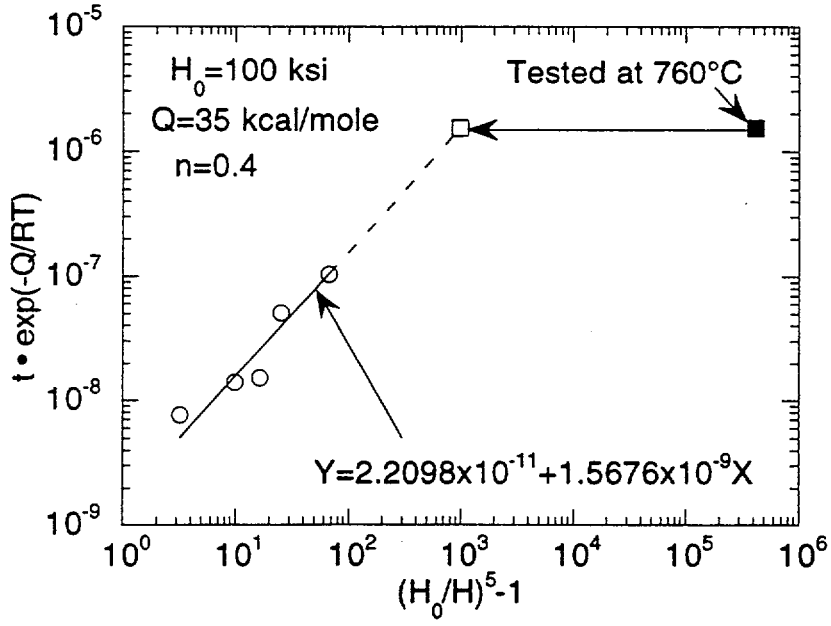

(b)

Fig. 9. Flow stress ("unaged") parameter vs. temperature plot for electrosleeve material. The data (open square symbol) at 760°C was estimated from the tensile data (filled square symbol) on a specimen aged and tested at 760°C, using a Hall-Petch exponent (a) n = 0.33 and (b) n = 0.40.

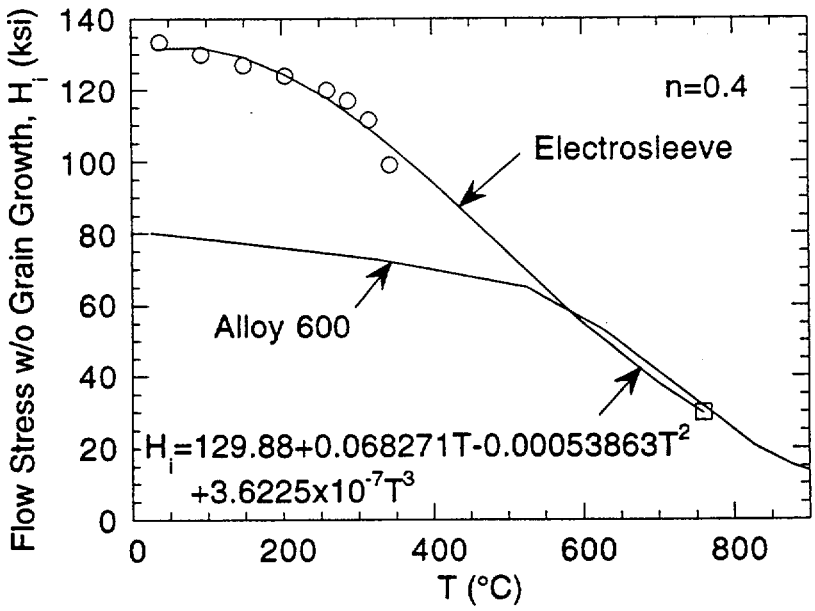

Fig. 10. Flow stress ("unaged") vs. temperature plot for electrosleeve material and Alloy 600. The Electrosleeve data (square symbol) at 760°C was estimated from tensile data on a single specimen pre-aged and tested at 760°C, using n=0.4.

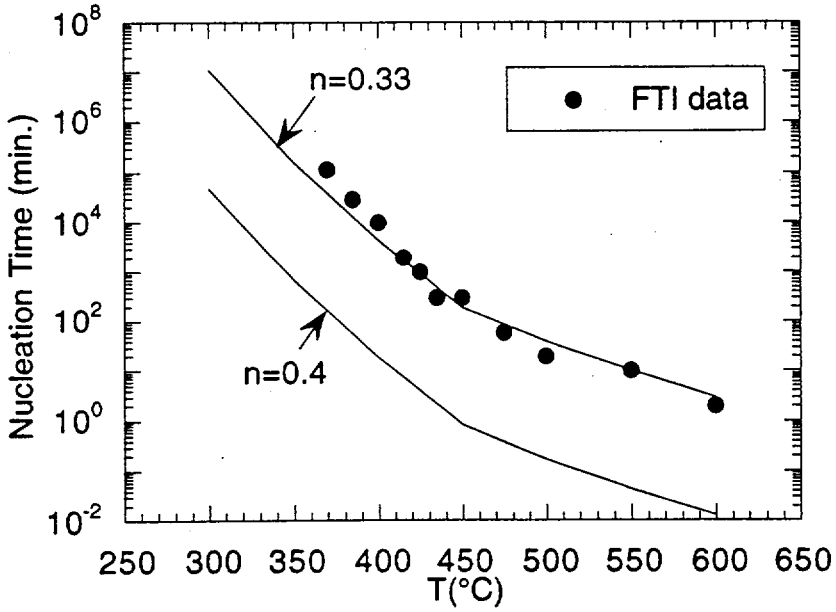

Fig. 11. Variation of calculated "nucleation" times to onset of rapid loss of flow stress (or grain growth) under isothermal aging with aging temperature for Hall-Petch exponents of n= 0.33 and n = 0.40, using a temperature-dependent activation energy given by the step function in Fig. 6. Also shown are nucleation times for rapid loss of flow stress derived from the FTI data shown in Fig. 5.

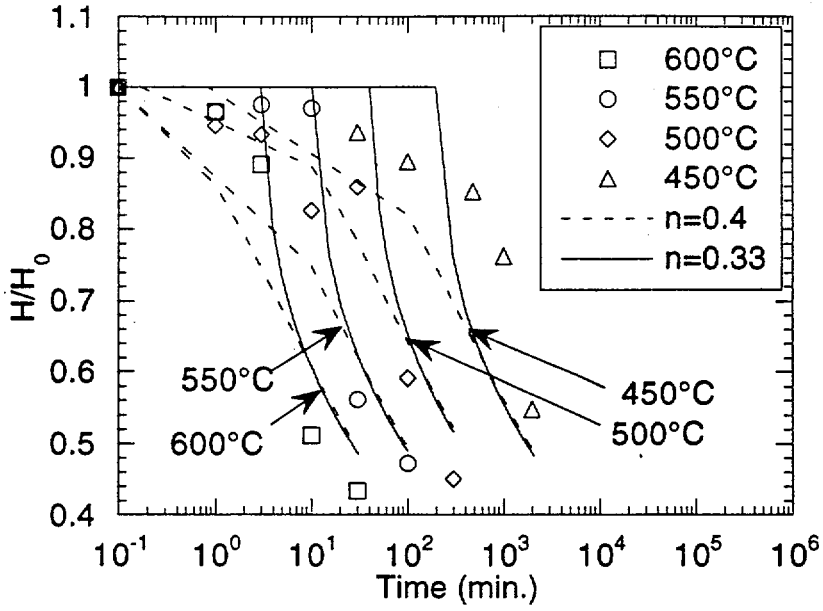

Fig. 12. Comparison of the calculated variations of normalized Vickers Hardness Number (VHN) of the Electrosleeve, using the Hall-Petch model with n=0.33 and n=0.4. with the experimentally measured variations under isothermal aging at various temperatures.

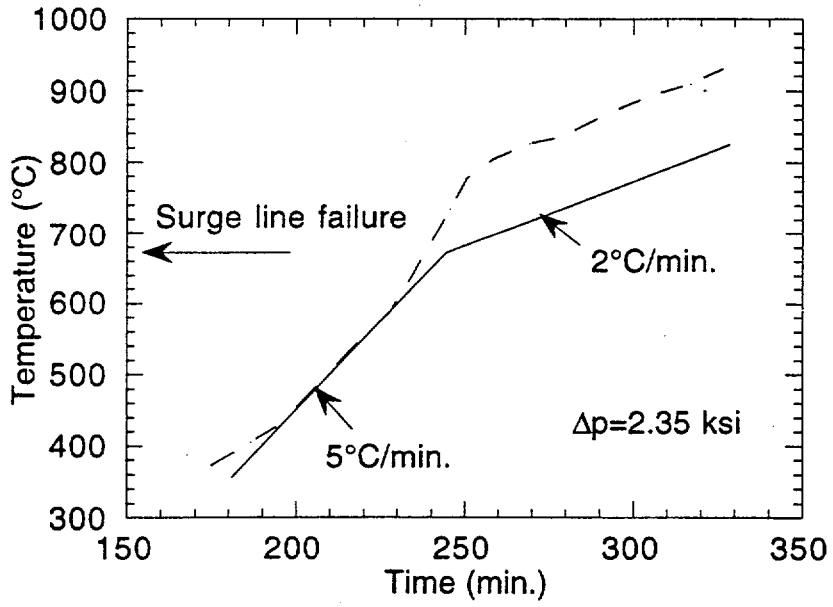

Fig. 13. Time-temperature history for tests reported in NUREG-1570 (dashed line) and simplified scoping ramp (solid line).

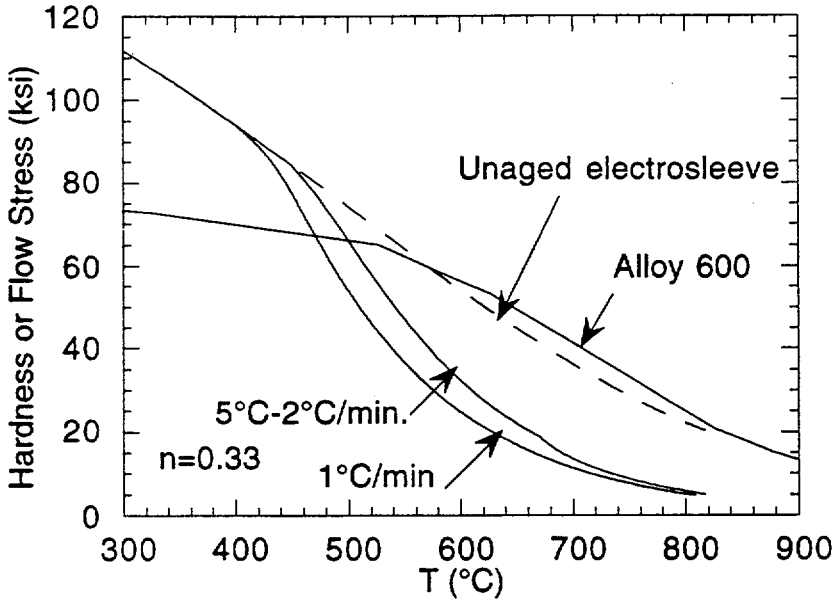

(a)

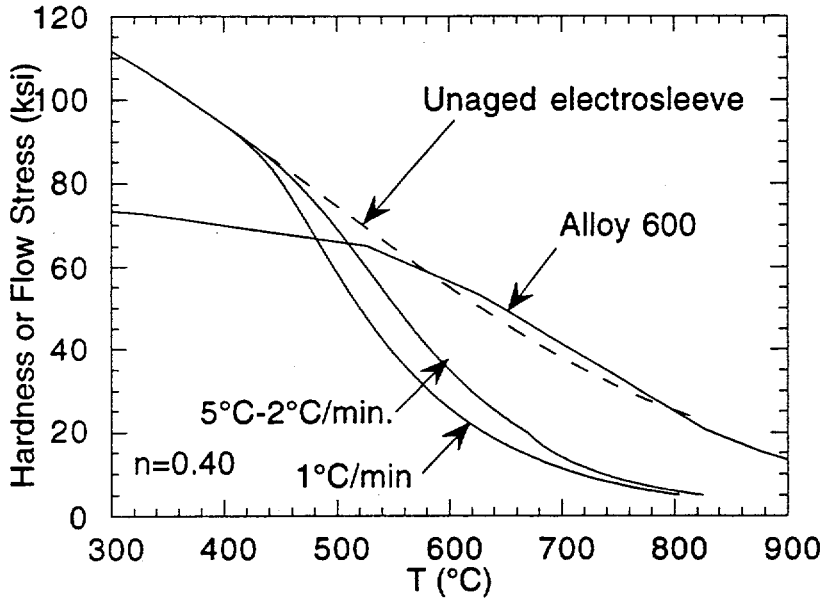

(b)

Fig. 14. Calculated reductions of flow stress of the electrosleeve material with temperature, using Hall-Petch exponent (a) n=0.33 and (b) n=0.40, for two temperature ramps.

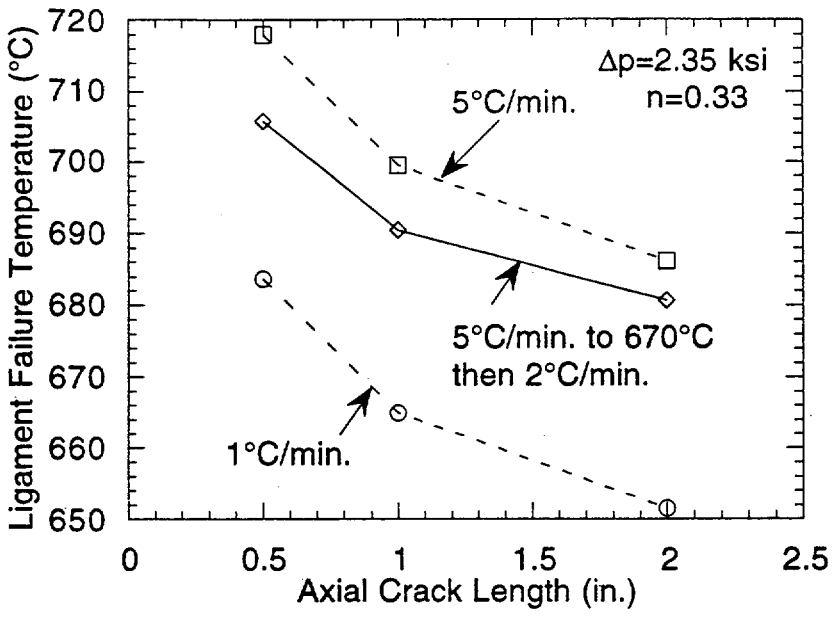

(a)

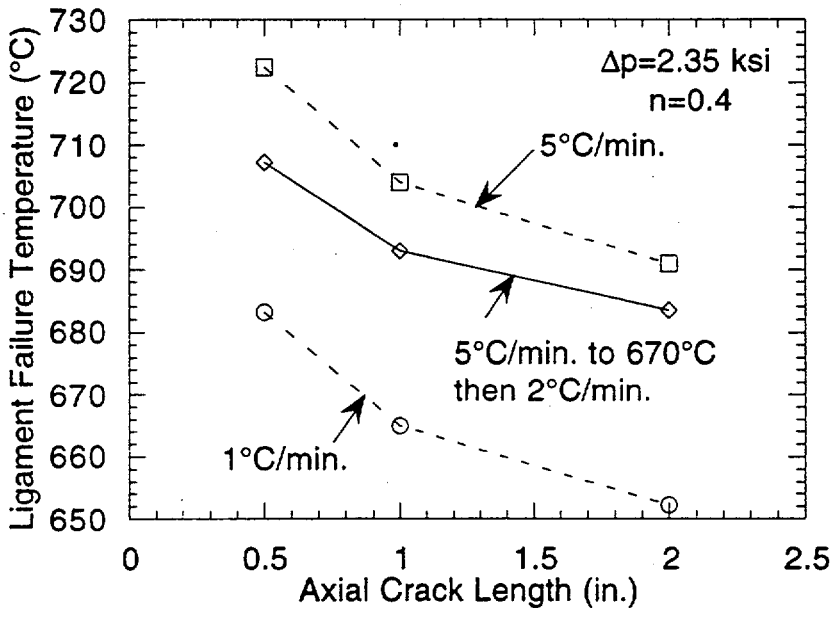

(b)

Fig. 15. Predicted ligament failure temperatures by the Hall-Petch model for Electrosleeved tubes with throughwall axial cracks under various temperature ramps, using (a) n = 0.33 and (b) n = 0.4.

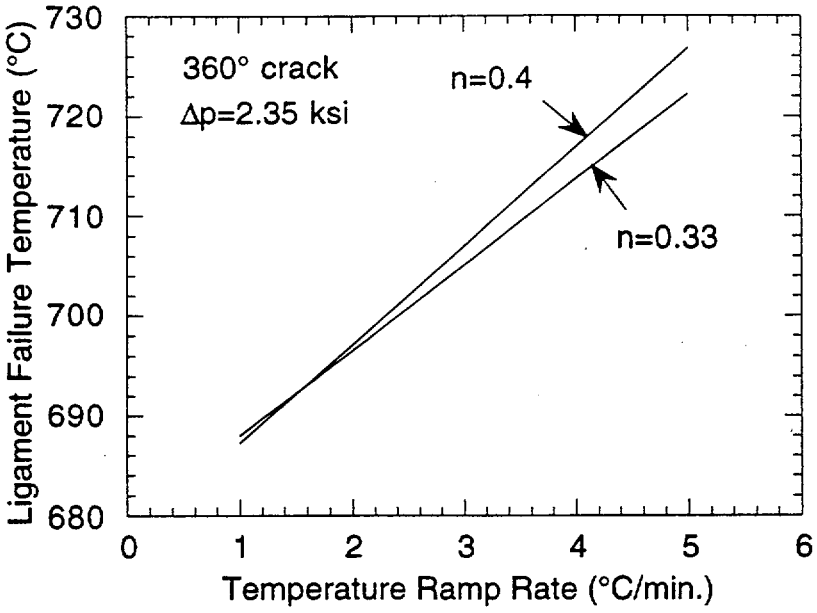

Fig. 16. Predicted ligament failure temperatures by the Hall-Petch model for Electrosleeved tubes with a throughwall 360° circumferential crack under various temperature ramps.

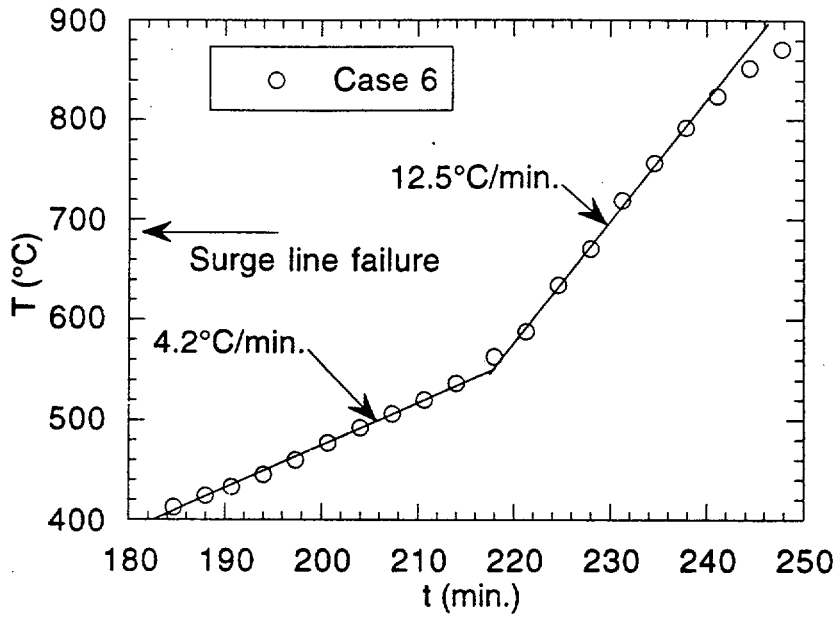

(a)

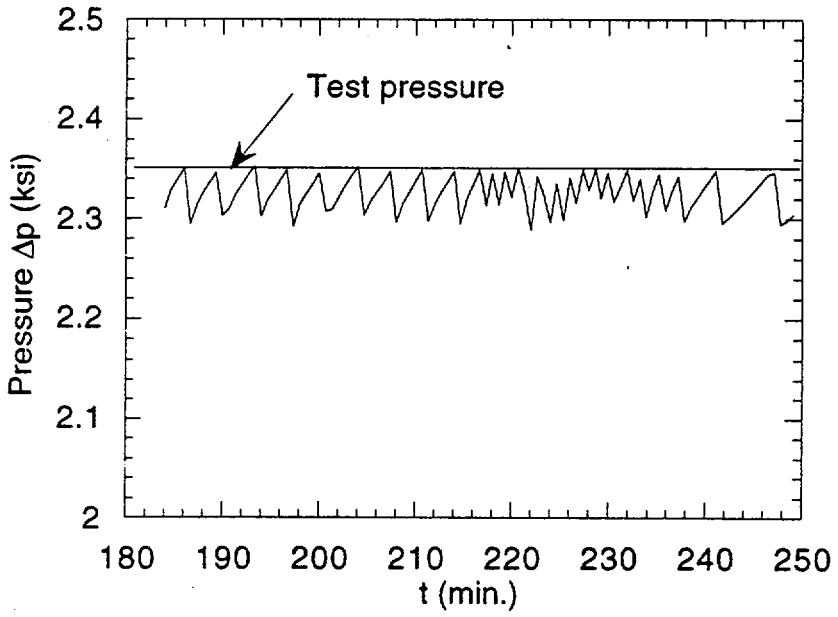

(b)

Fig. 17. Calculated variation and ANL test simulation of (a) temperature and (b) pressure differential during an SBO (case 6) severe accident transient.

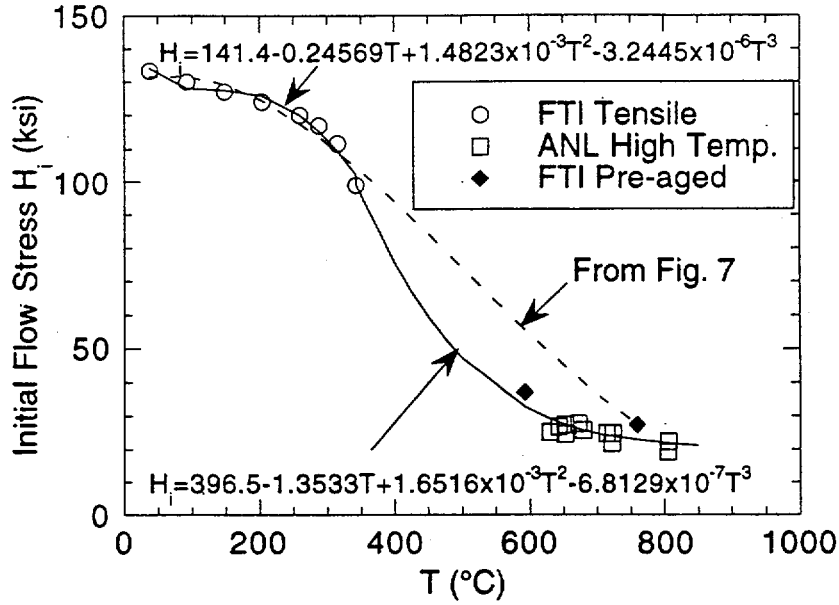

Fig. 18. Original unaged flow stress curve (dashed line) of the Electrosleeve estimated from FTI tensile data before the ANL tests were conducted and revised unaged flow stress curve (solid line) of the Electrosleeve calculated using the ANL tests.

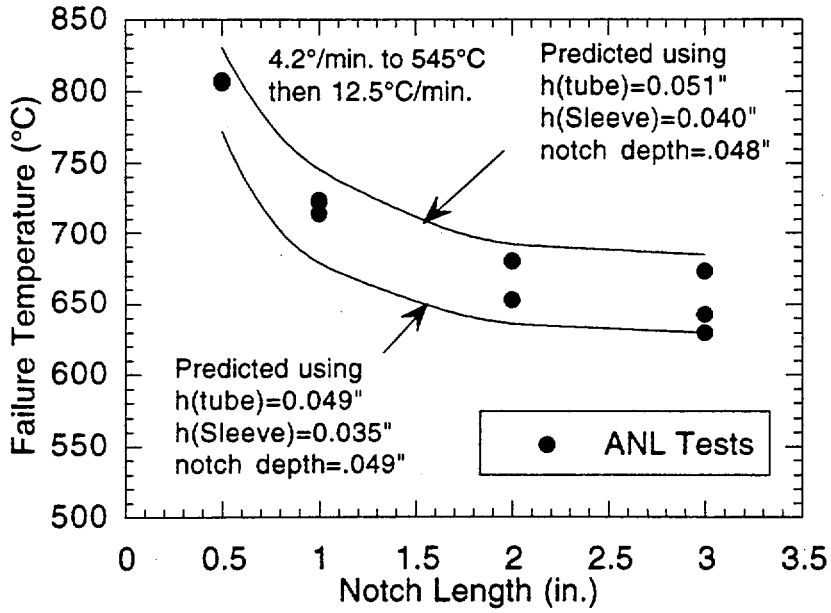

Fig. 19. Variation of ANL test failure temperatures and predicted upper and lower bounds to the failure temperatures with notch length.

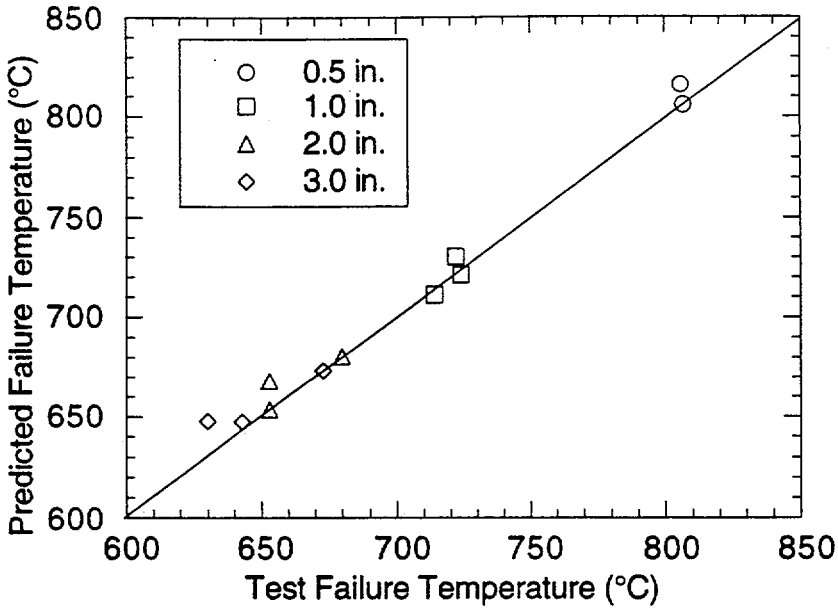

Fig. 20. Predicted vs. observed failure temperatures of the ANL tests.

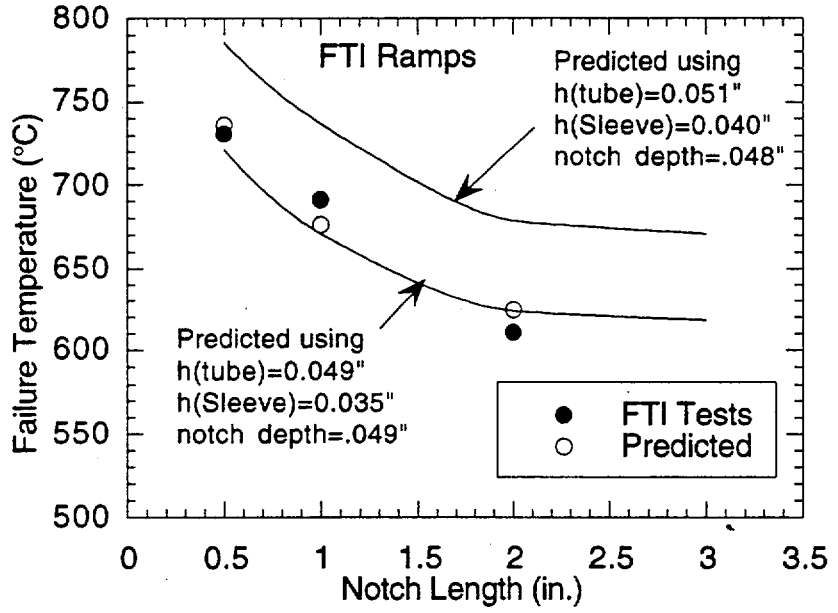

Fig. 21. Predicted vs. observed failure temperatures of the FTI tests. The predicted points are based on actual geometry and actual temperature ramp for each specimen.

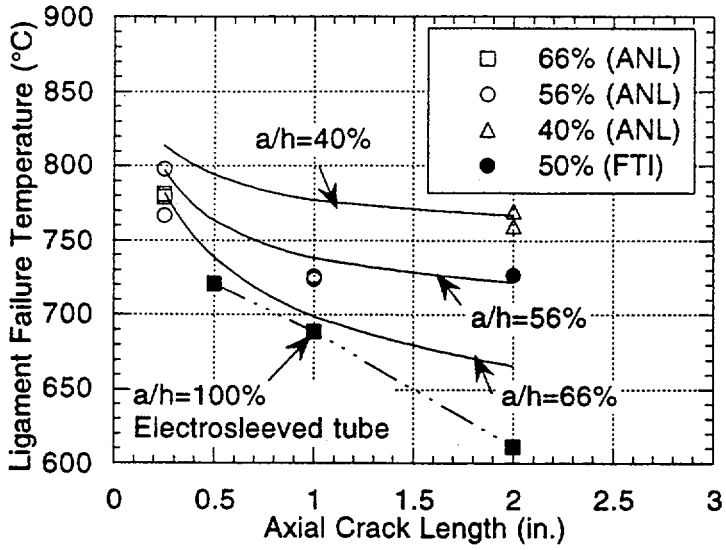

Fig. 22. Comparison of experimental ligament failure temperatures (from NUREG/CR-6575) with predicted values (using flow stress model) for unsleeved Alloy 600 tube with part-throughwall axial cracks under EPRI ramp. Also shown are FTI data for an unsleeved tube with a 2 in./50%TW crack (filled circle) and Electrosleeved tubes (filled squares) with throughwall cracks in the parent tubes.

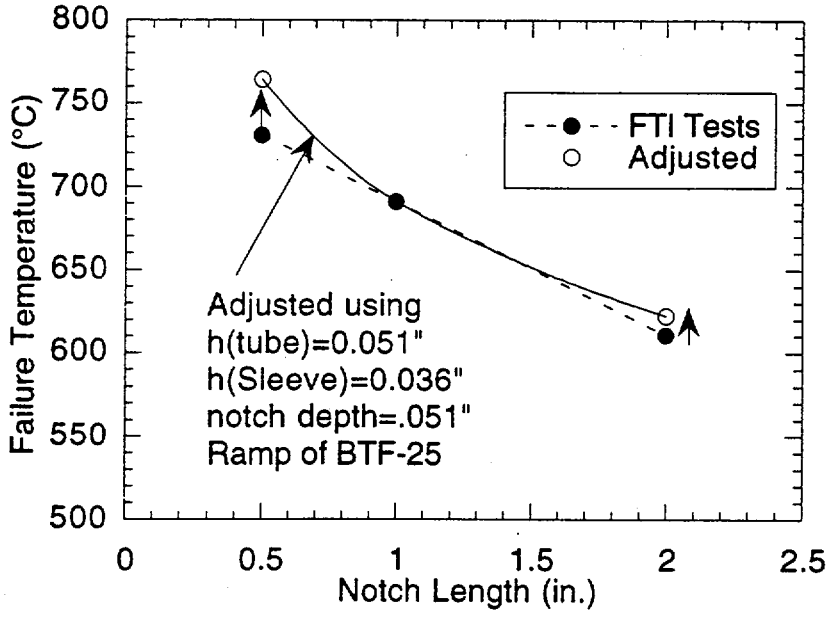

Fig. 23. Comparison of FTI test failure temperatures for the Electrosleeved tubes with adjusted values that are obtained by using the flow stress model so that all specimens have identical geometry (that of BTF-25) except the notch length and are subjected to the same temperature ramp as BTF-25.

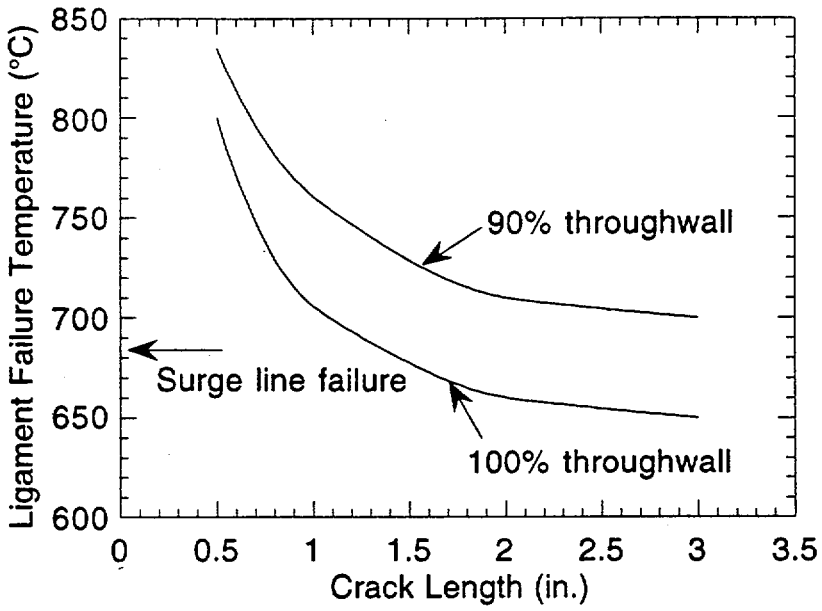

Fig. 24. Predicted ligament failure temperature during the SBO severe accident Case 6 (see Figs. 18a-b) vs. crack length for 90% and 100% throughwall cracks in the parent tube. Also shown is the tube temperature at the time of surge line failure.

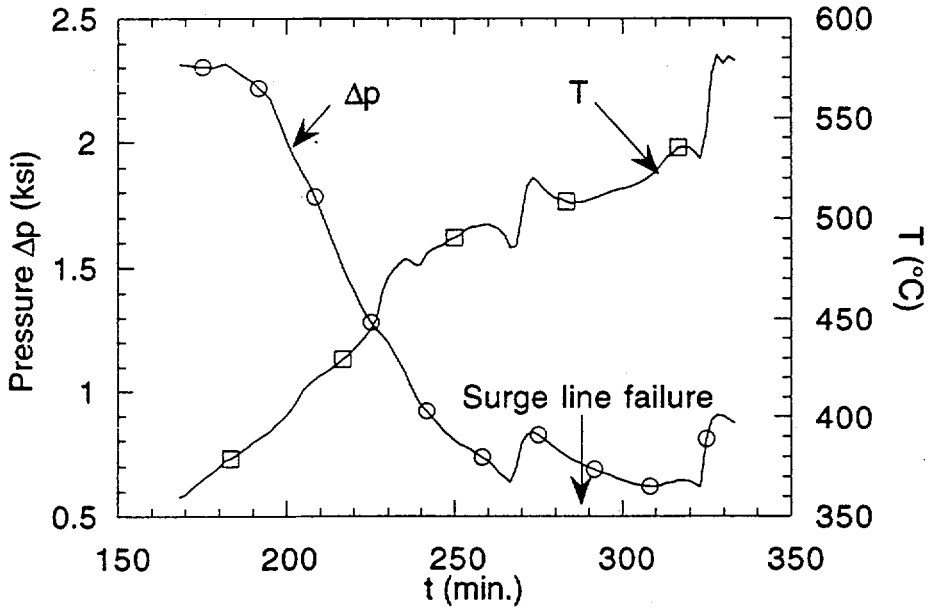

Fig. 25. Variation of temperature and pressure during SBO with pump seal leak(case 20C) severe accident transient.

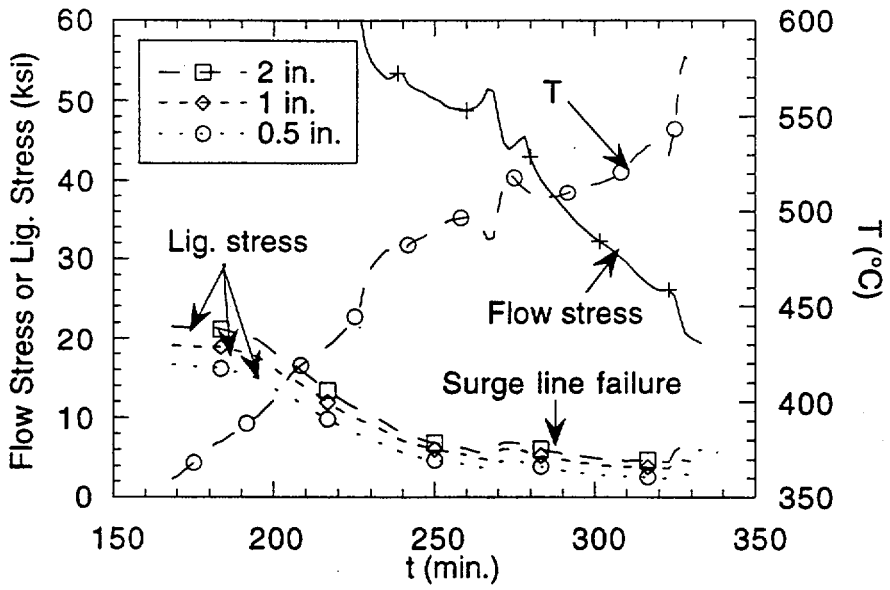

Fig. 26. Time variations of temperature, flow stress of the Electrosleeve, and average ligament stresses predicted for 100% throughwall cracks of length 0.5 in., 1 in., and 2 in. in the parent tube during the severe accident Case 20C (SBO with pump seal leak). The flow stresses for times less than ≈228 minutes are > 60 ksi. Note that the ligament stresses are well below the flow stress up to surge line failure.

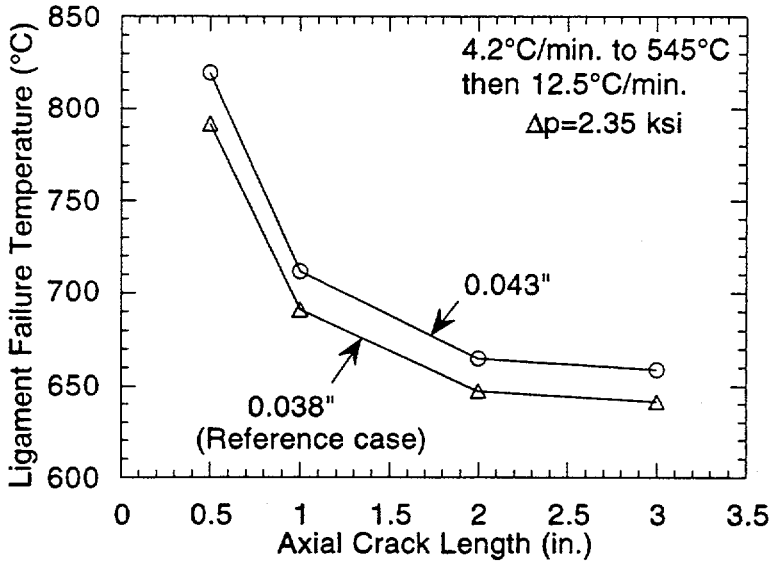

Fig. 27. Effect of Electrosleeve thickness on the predicted ligament failure temperature of a tube with throughwall axial cracks.

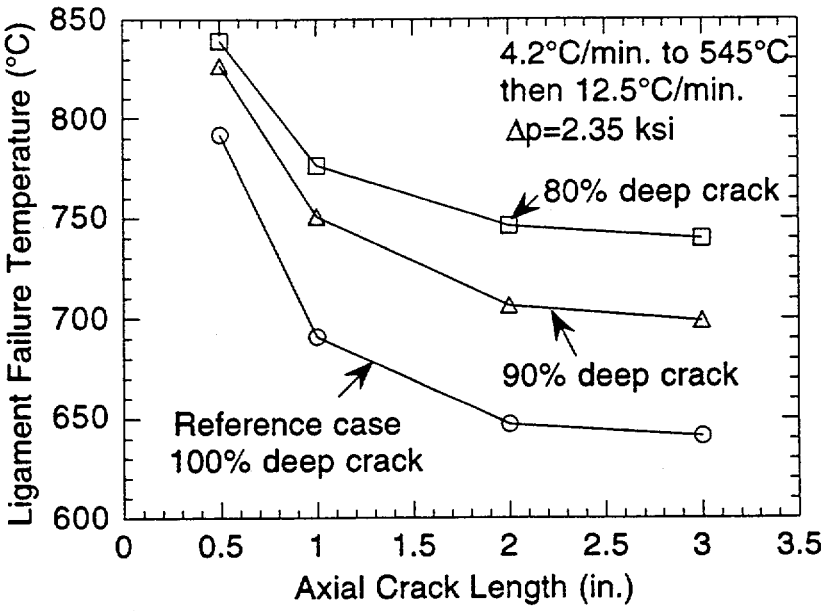

Fig. 28. Effect of changes in crack length and depth on the predicted ligament failure temperature, using area weighted flow stress of ligament for calculating both the effective m_p and failure temperature.

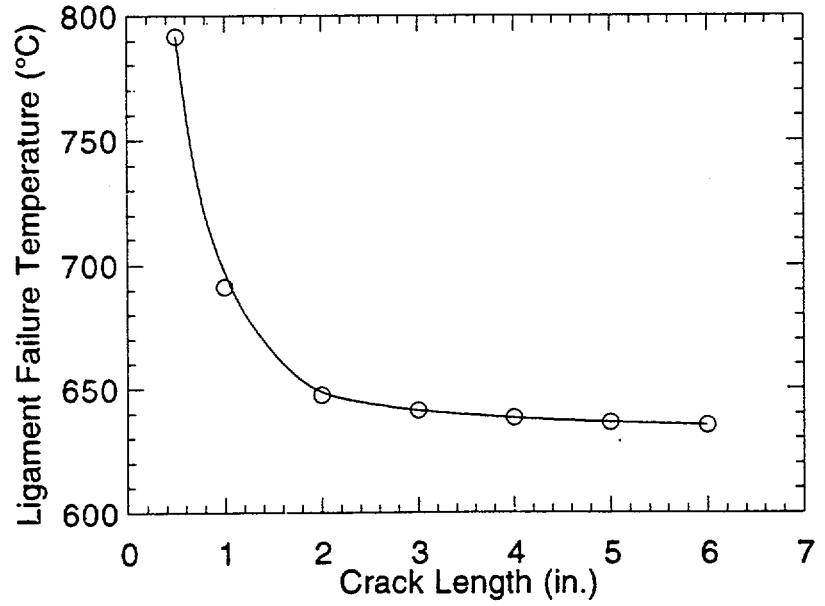

Fig. 29. Effect of crack length on the predicted ligament failure temperature of the reference Electrosleeved tube with throughwall axial cracks in the parent tube during the Case 6 SBO severe accident ramp.

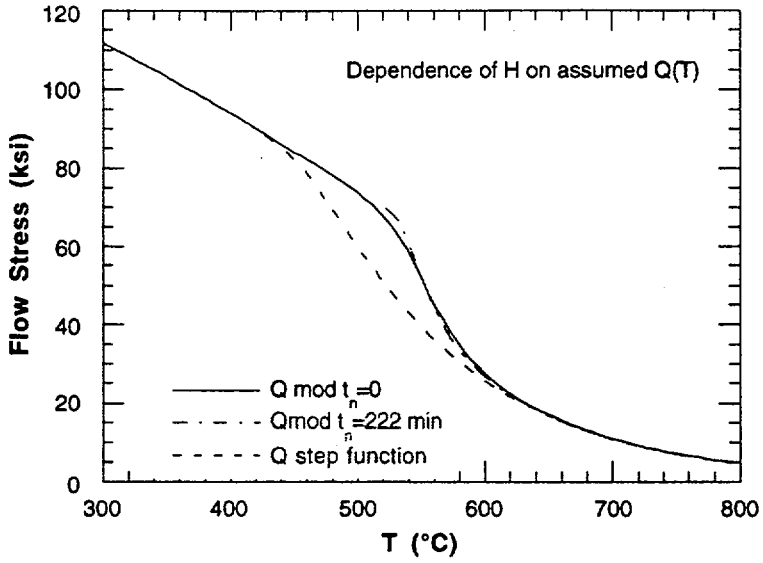

Fig. 30. Effect of the shape of the variation of activation energy with temperature on the calculated loss of flow stress for a 1°C min ramp. Note also that the nucleation time has little effect on the flow stress at the temperatures of interest.

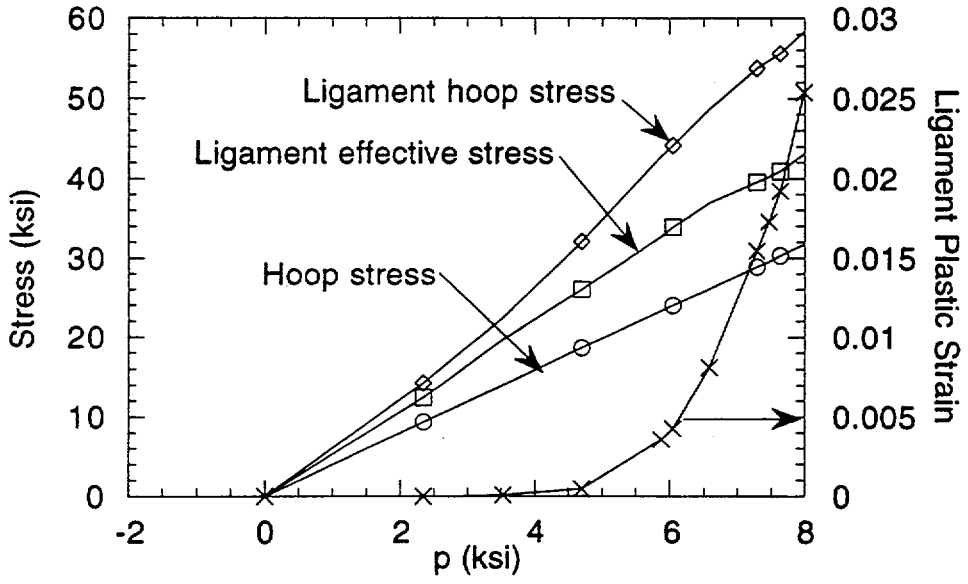

Fig. 31. Variations of the average hoop stress, average effective stress, and average hoop plastic strain in the ligament with pressure as calculated from FEA results for a homogeneous tube of wall thickness 0.088 in. that contains a 3 in. long, 0.050 in. deep part-throughwall axial crack. Also shown is the variation of the average hoop stress in an unflawed tube with pressure.

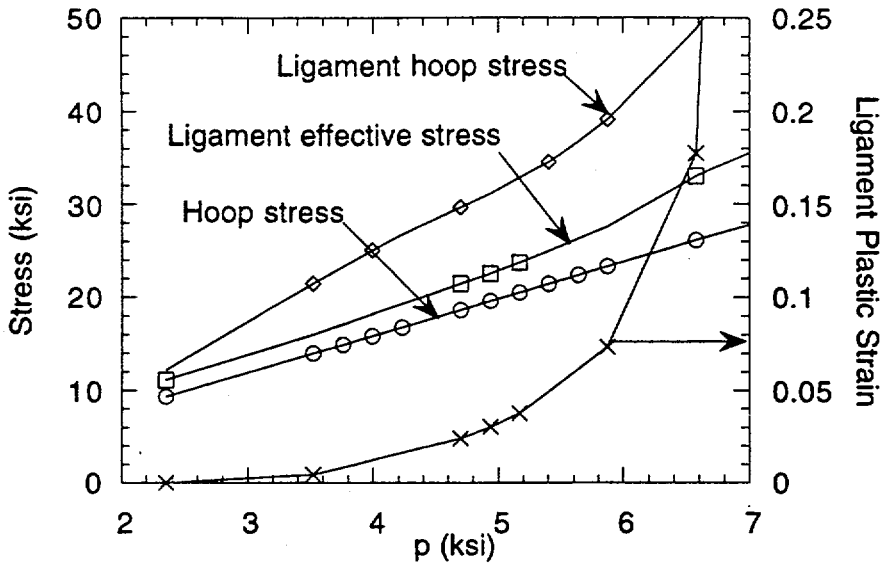

Fig. 32. Variations of the average hoop stress, average effective stress, and average hoop plastic strain in the ligament with pressure as calculated from FEA results for a bi-layer tube (simulating an Electrosleeved tube at high temperature) with a 0.038 in. thick inner layer and a 0.050 in. thick outer layer that contains a 3 in. long, 100% throughwall axial crack. The flow stress ratio between the outer and the inner layer=2. Also shown is the variation of the average hoop stress in an unflawed tube with pressure.

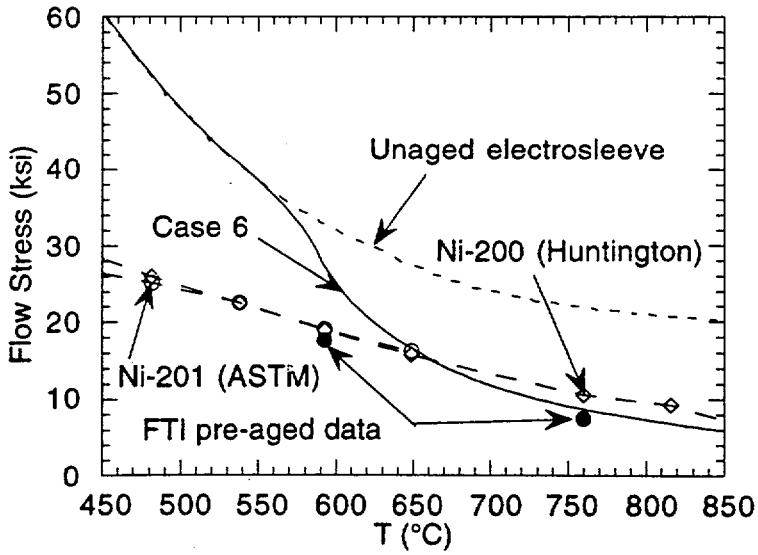

Fig. 33. Comparison of calculated flow stresses (including aging) of Electrosleeve (solid line) with flow stress data (open symbols) of Ni 200 (Huntington) and Ni-201 (ASTM). Also shown are the flow stress of the unaged electrosleeve (short dashed line) and two FTI flow stress data (filled circle) on 30-min aged specimens.